Power curve measurement with a sector scanning lidar from the TP and a nacelle lidar at Greater Gabbard

Wagner, Rozenn; Vignaroli, Andrea; Gómez, Paula

Publication date:
2015

Document Version
Publisher's PDF, also known as Version of record

DTU Wind Energy GG I-0016 (EN)

Power curve measurement with a sector scanning lidar from the TP and a nacelle lidar at Greater Gabbard

Deliverable D5.3
Version 1.2

Rozenn Wagner, Andrea Vignaroli (Authors)
Paula Gomez (Review)

DTU – Wind Energy
Risø Campus
Roskilde, Denmark
June 2015

Preface

This document is deliverable D5.3 of the project Greater Gabbard Offshore Wind Farm - IPCT and LiDAR Equivalent IPCT according to Contract Nr. 13.0586. This project aims at assessing whether a lidar placed on the nacelle or the transition piece of an offshore wind turbine could be used for power curve verification instead of a met mast. This report presents the results obtained with both the TP scanning lidar and the nacelle lidar for a concurrent datasets.

Total number of pages: 48

Version number	Date	Author/editor	Change
1.1	15 June 2015	Rozenn Wagner	Version 1
1.2	11 October	Andrea Vignaroli	Version 1.1

Name and address of client:

Greater Gabbard Offshore Winds Ltd
c/o SSE Ltd
One Waterloo Street
Glasgow
G2 6AY
UK

Name and address of measurement laboratory:

DTU Wind Energy
Building 118
P.O. Box 49
Risø Campus
Frederiksborgvevj 399
DK-4000 Roskilde
Denmark

Abstract

Nacelle lidars have been demonstrated to be useful for power curve measurement. Scanning lidars have shown promising results for onshore tests. In this project, a power curve measurement was carried out on an offshore wind turbine with both a nacelle mounted lidar and a scanning lidar placed on a wind turbine transition piece. A two-beam Wind Iris lidar was installed on the nacelle of the wind turbine and measured the horizontal wind speed at 2.5D upstream. Simultaneously, a WINDCUBE 100S was placed on the west side of the turbine, on the transition piece. Prior to their deployment offshore, both lidars were calibrated by DTU at their testing facility at Høvsøre, Denmark. These calibrations provided the essential basis to quantify the lidars' measurement uncertainties; thus allowing a meaningful comparison of the lidar measurements to the met mast offshore, in terms of wind speed and power output.

The Wind Iris nacelle lidar was measuring between 1m and 3m above hub height; this corresponds to 1.3% to 3.8% of hub height, which is exceeding the requirements of the IEC 61400-12-1 to measure at hub height +/-2.5%. This deviation is believed to be due to challenging configuration of the optical head inclination while the turbine nacelle was moving a lot. If we had managed to incline the optical head by the desired pre-tilt angle (0.76°), the beam would have been within the required range. Nevertheless, since the vertical wind shear was rather low during this measurement campaign, the sensing height error did not significantly affect the lidar 10 minute mean wind speed measurement.

Regarding the WINDCUBE 100S, one of the main challenges has been to set up the lidar beam elevation angle to measure just above the cup anemometer (in order to avoid the strong backscatter that could be returned if the beam was hitting the cup anemometer or the mast). First estimations based on the wind turbine and mast GPS positions and the height of the mast and turbine transition pieces resulted in an elevation angle that was too small to reach the top of the mast. This has been adjusted by performing several sector scans (PPI scans) with various elevation angles in order to find the top of the mast. Thanks to this approach we are sure that the beam is scanning within 2m above the cup anemometer. The difference between the estimated scanning head elevation angle and the actual one is expected to be due either to a discrepancy between the designed and installed turbine and/or met mast platforms (being either vertically or horizontally offset) or to mechanical problem in the lidar scanner head that would have occurred during transportation to the offshore site.

The tilting of the turbine transition piece due to the turbine tower bending under various thrust loads on the rotor, has also been shown to be significant. The inclinometer measurements from the lidar showed that the beam height was varying by +/-0.75m around the mean height depending on the wind direction and the wind speed. Nevertheless the amplitude of the tilting of the transition piece is clearly smaller than for the nacelle, meaning that the WINDCUBE 100S beam remained within a smaller height range than the nacelle lidar.

The reconstructed 10 minute wind speed from both lidars compared fairly well to the measurements from the mast top mounted cup anemometer. The WINDCUBE 100S has been measuring 0.23% higher that the cup anemometer (at 10m/s) and the scatter increases as the wind speed increases; whereas the Wind Iris wind speed was larger than the cup wind speed by 0.34% for a wind speed of 10m/s.

The power curves obtained with the lidars were very similar to the cup anemometer power curve and the lidars derived AEP were lower than the cup anemometer derived AEP, by 0.39% with the WINDCUBE 100S and by 0.32% with the Wind Iris (for an annual average wind speed of 8m/s).

The category A uncertainty in power obtained with the WINDCUBE 100S is slightly larger than that obtained with the mast top mounted cup anemometer, because of the larger scatter. On the other hand, the category A uncertainty in power obtained with the Wind iris is slightly smaller than that obtained with the mast top mounted cup anemometer, due to the fact the nacelle lidar is always measuring upwind, compared to the met mast which has a fixed position for a rather large wind sector.

The category B uncertainty in wind speed obtained with both lidars is higher than that resulting from the standard set up with the top mounted cup anemometer, mainly because of the large sensing height error. The latter uncertainty has been derived from a maximum deviation obtained by assuming a generic maximum shear coefficient of 0.5. This is a rather conservative approach; the shear

exponent measured with the mast over the lower half of the rotor was 0.05 on average. The inclinometer uncertainty has a quite marginal contribution.

The total power curve uncertainty is the combination of the category A uncertainty and the various category B uncertainties (wind speed, temperature and pressure). The power curve uncertainty is dominated by the category B uncertainty in wind speed. The total power curve uncertainties obtained with both lidars were therefore larger than that obtained with the mast top mounted cup anemometer. The Wind Iris power curve uncertainty is smaller than the WINDCUBE 100S power curve uncertainty. In both cases, the difference between lidar and cup power curve remains relatively small compared to the total power curve uncertainty.

Contents

1. Introduction

Nacelle lidars have been demonstrated to be useful for power curve measurement [1]. Scanning lidars have shown promising results for onshore tests [2]. In this project, a power curve measurement was carried out on an offshore wind turbine simultaneously with a nacelle mounted lidar and a scanning lidar placed on the wind turbine transition piece. A two-beam Wind Iris lidar was installed on the nacelle of the wind turbine and measured the horizontal wind speed at 2.5D upstream. Simultaneously, a WINDCUBE 100S was placed on the west side of the turbine, on the transition piece (TP) platform. A met mast compliant to the IEC 61400-12-1 requirements [3], located at about 2.5D from the wind turbine, has been used as a reference to assess the performance of the lidars for power curve verification.

Prior to their deployment offshore, both lidars were calibrated by DTU at their testing facility at Høvsøre, Denmark. The 2-beam Wind Iris nacelle lidar was calibrated according to the procedure previously developed by DTU [4]. The radial wind speed (RWS) was compared to a reference cup anemometer along each line of sight (LOS) separately. They were combined to provide the uncertainty in the horizontal wind speed measurement which was lying between 1.7% and 2.9% [5]. In this project the reconstruction algorithm from the horizontal wind speed was developed by Leosphere and applied by DTU as a black box. The calibration of the WINDCUBE 100S was therefore performed with a “black box” approach. The lidar was placed at 250m from a met mast mounted with a top cup anemometer at 99.5m. 45° sector scans were performed right above the cup anemometer. The lidar reconstructed 10 min mean wind speed was calibrated against the 10 min mean wind speed given by the cup anemometer. The lidar horizontal wind speed measurement uncertainty varies between 1.9% and 2.9% [6].

Both lidars were equipped with inclinometers in order to monitor their motion due to the turbine (nacelle and transition piece) movement, during the measurements. Those inclinometers were also calibrated while the instruments were at Høvsøre.

This report describes the results from the analysis of the measurements taken with the Wind Iris nacelle lidar and the WINDCUBE 100S, installed on the wind turbine IGF10 in the Greater Gabbard wind farm, between January and April 2015. The site, the measurement set up and the dataset collected are first described. Secondly, the performances of each lidar are discussed. Finally the power curves measured with the two lidars are compared to the met mast power curve in terms of AEP and uncertainty. The lidar wind speed measurement uncertainties estimated with the calibration of the devices were used as basis for the total power curve uncertainty budget estimation.

2. Site description

The Greater Gabbard wind farm is located in the North Sea about 23 km from Lowestoft, Suffolk, UK (see Figure 1). Figure 2 shows the wind farm layout and the position of turbine IGF10, on which the lidars were installed. The photographs in Figure 3 to Figure 6 show the horizon around the test turbine, starting from North-East and turning clockwise. The only relevant obstacles (within a distance of 20D or 2140m) are the 4 turbines: IGE13, IGE14, IGF09 and IGG11. A sketch displaying the relative positions of those turbines to IGF10 and the met mast is shown in Figure 7.

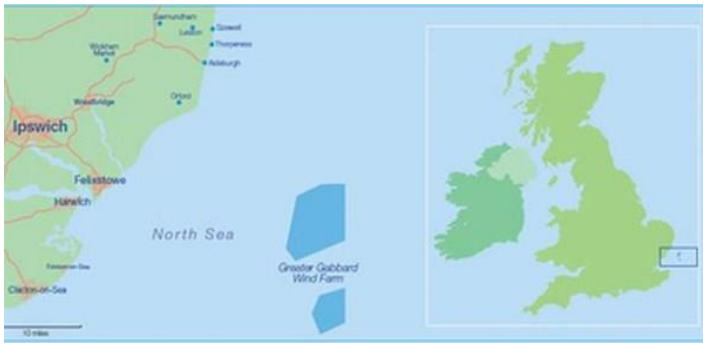

Figure 1 Relative position of the Greater Gabbard Wind Farm

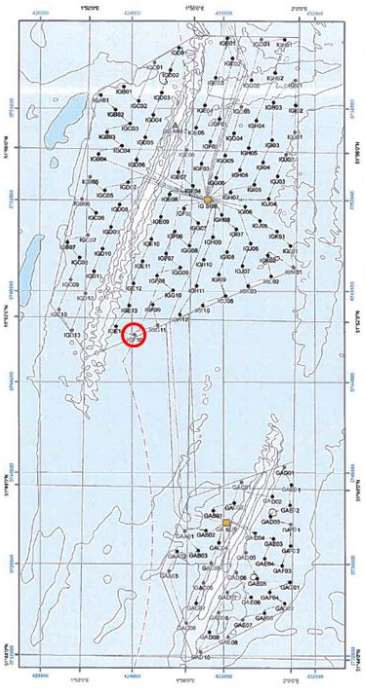

Figure 2 Layout of the Greater Gabbard Wind Farm. The position of wind turbine IGF10 is shown with a red circle.

Figure 3 View from turbine IGF10: North – East

Figure 4 View from turbine IGF10: East

Figure 5 View from turbine IGF10: South – West

Figure 6 View from turbine IGF10: North – West

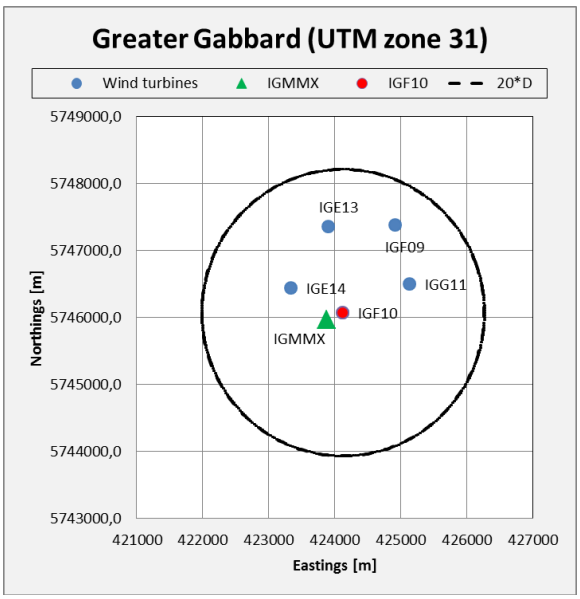

Figure 7 Relative positions of wind turbines within 20D around IGF10 (red dot) and met mast (green triangle)

Table 1 Coordinates and rotor diameters of the wind turbines in the vicinity of the tested turbine

	Coordinates (UTM 32 ED50)		D_n
	E (m)	N (m)	(m)
IGE13	423903.4	5747356.6	107
IGE14	423332.2	5746440.8	107
IGF09	424918	5747386.9	107
IGG11	425130.8	5746503.1	107

3. Measurement set up

3.1 Wind turbine

The wind turbine is a pitch-regulated Siemens 3.6MW, with a rotor diameter of 107m and hub height of 79.5m above CD. The foundation is a monopile. The transition piece of the wind turbine is at 14.890 m above CD [7].

The turbine generates 690V which is stepped up to 33kV for inter-array transmission and then up to 132kV at the offshore substation for transmission back to the onshore substation.. The grid is part of the European grid, which is very strong. It is considered that the voltage variations are lower than 1.5%, and frequency variations are lower than 0.1 Hz.

The electrical power was measured with Noratel Garre current transformers (3 pieces), with a class of 0.2S, installed in the TPPI kit at the transition piece level.

3.2 Met mast

The met mast used as reference in this measurement campaign was positioned at a distance of 267m from turbine IGF10 with a bearing of 247°. Its instrumentation was compliant to the requirements of the IEC 61400-12-1 for power curve verification, including a top mounted Wind sensor anemometer at 79.5m CD, as well as a wind vane at 77.6m, a barometric air pressure sensor [3], a temperature sensor and a humidity sensor that were used to correct the wind for air density in the power curve analysis. A sketch and picture of the met mast are given in Figure 8 and Figure 9, respectively. The transition piece of the met mast is 15.0m above CD [8]. Table 2 provides the details of the instrumentation.

Table 2 List of measured parameters

Parameter	Sensor	Transducer	Position*
Wind speed at hub height (Vhub)	Risoe Cup Anemometer Type: P2546A sn.: 16890,	Included	Met mast Height 79.59m
Wind speed at 77.59m (Vref)	Risoe Cup Anemometer Type: P2546A sn.: 16891	Included	Met mast Height 77.59m
Wind direction	207 Wind Vane (potentiometer wind vane); manufacturer: Ornytion; sn. 207P0Z435139	Included	Met mast Height 77.59m
Temperature	Pt100 sensor P2449a sn.: 114.	Included	Met mast Height 77.59m
Atmospheric pressure	Vaisala PTB110 600-1100hPa. sn.: H4740010	Included	Met mast Height 77.59m
Relative humidity	HMP155 sn.: F4110030		Met mast Height 77.59m
Electrical power	Current transformer (3 pieces): Brand: Noratel Garre Type: LGK-2 4000/1A 40VA C, Class 0.2S (sn: 12/826536, 12/826537, 12/826538)	Brand: Camille Bauer Type: Sineax Cam (sn: 130/684080, Trescal no: 258704), analogue output (Class 0.5) Input/output range @ 230 V: -750kW … 0 ... +4600 kW	Tower bottom

Status signal K3 “Generator running”	Signal from control system	Included	Tower bottom
Status signal K4 “Turbine. Available”	Signal from control system	Included	Tower bottom
Status signal K5 “Power reduced”	Signal from control system	Included	Tower bottom

* All sensor positions are given above sea level (chart datum).

*Sensor positions are given above CD.

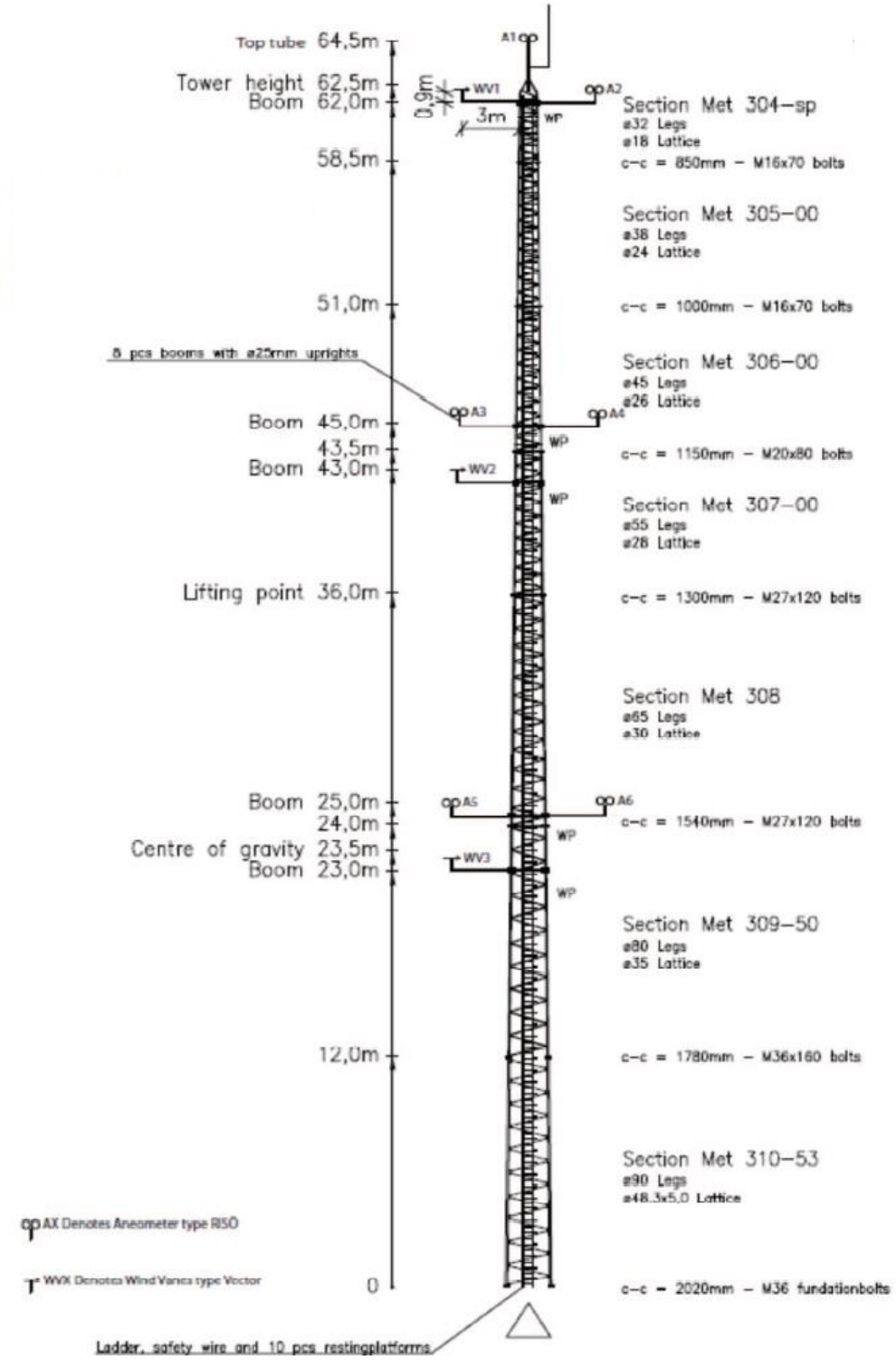

Figure 8 Principle sketch of met mast instrumentation; the lightning finial was removed on 7th of August 2014; the instrument orientation for the anemometers is 115 Deg and for the wind vanes it is 295 Deg

Figure 9 Photo of the met mast

3.3 Measurement system

The measurements have been performed using SSE and Siemens equipment. DTU has approved the measurement setup and performed the data analysis.

The measurements from the met mast were logged by two data loggers – Campbell Scientific CR3000. The measurements from the wind turbine were logged by one data logger – Campbell Scientific CR1000.

The gains and offsets applied to the measurement channels of the two Campbell Scientific CR3000 loggers can be found in [8].

3.4 WINDCUBE 100S

The WINDCUBE 100S is a scanning pulsed LiDAR system using Plan Position Indicator (PPI), Range Height Indicator (RHI) and DBS scanning techniques to picture 2D ambient flow fields, as well as wind profiles. With a range gate resolution of 50 m the device can measure to a distance of 3 km from the instrument.

In this measurement campaign, the WINDCUBE 100S was used to perform sector scans (PPI) over 45° right above the met mast top mounted cup anemometer. One scan duration was about 15 seconds and the radial wind speed was measured along 30 lines of sight. The algorithm to reconstruct the 10 minute mean horizontal wind speed and direction was developed by Leosphere and provided to DTU as an executable file, which was run as a black box.

Furthermore, the WINDCUBE 100S used in this measurement campaign was equipped with extra inclinometers (identical to those used in the Wind Iris), in order to monitor the tilting and rolling of the lidar on the turbine transition piece during the measurements.

3.4.1 Lidar position

The WINDCUBE 100S was installed on the turbine transition piece platform, as shown in Figure 10 and Figure 11, in July 2014. Ideally the lidar would have been placed directly in front of the met mast. However, an oil bursting exhaust is located at 2m above the TP platform at this bearing, which could have possibly resulted in having the lidar covered with hot oil. The current position of the lidar is a compromise so it is at some distance from this exhaust and minimizes the impact in case of oil bursting and making sure the beam is not obstructed by any obstacle while performing an arc scan centered on the mast position. The lidar scanning head is 1.3 m above the TP platform.

The north reference of the lidar was offset 56° clockwise from the mast-turbine direction. This offset was taken into account in the configuration of the scanning pattern. The relative direction of the mast from the lidar was 304°.

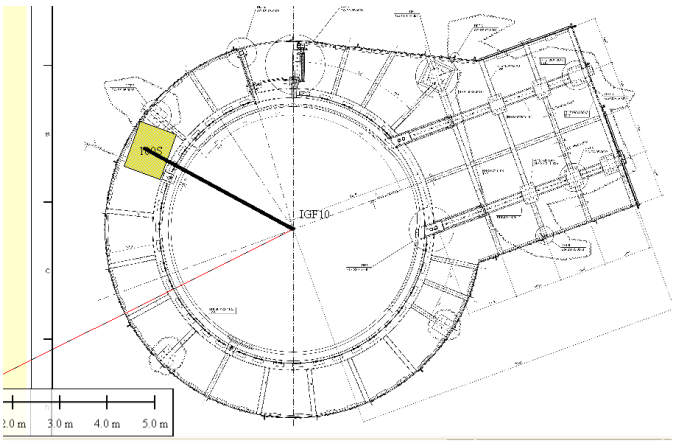

Figure 10 Top view sketch of turbine tower and transition piece platform and position of WINDCUBE 100S. The Lidar is represented by a yellow rectangle. North is towards the top of the figure. The red line shows the relative direction of the mast from the turbine.

Figure 11 Picture of WINDCUBE 100S after commissioning on the turbine transition piece platform. The scanning head of the lidar (middle of the window) was at 1.3m above the top of the transition piece railing.

3.4.2 Scanning head elevation angle

From the relative positions of turbine IGF10 and the met mast, and assuming the lidar was at 3.6m from the center of the turbine tower, it was estimated that the distance between the lidar and the met mast was 264.9m. The lidar beam should reach the cup anemometer height for an elevation angle of 13.4° and a range of 272m.

A couple of PPI and RHI test scans were performed with the W100S on the 8th of July. A Plan Position Indicator (PPI) scan is a scan where the laser beam elevation angle is fixed and the azimuth position is varying. A Range Height Indicator (RHI) scan is scan where the azimuth position of the laser beam is fixed while the elevation angle is varying (see Figure 12).

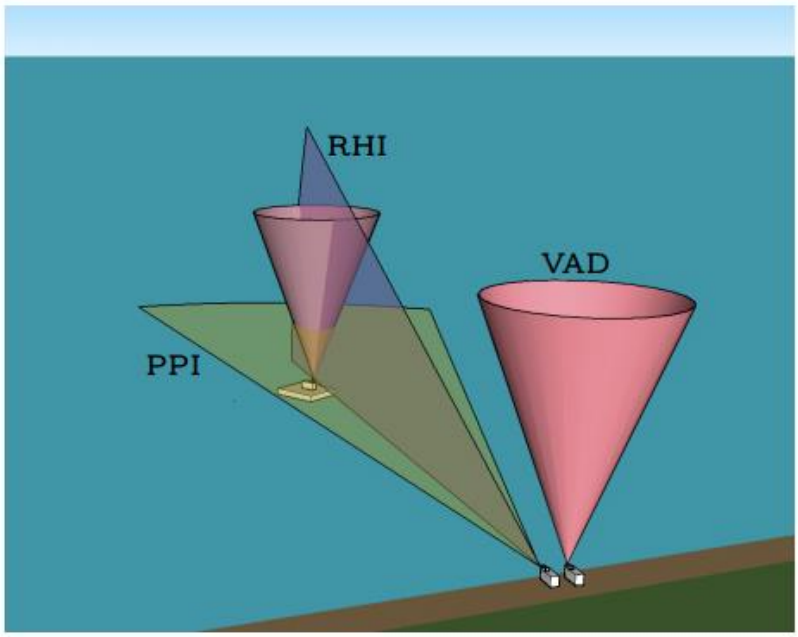

Figure 12 Typical measurement scenarios with a scanning lidar: PPI scan, RHI scan and Velocity Azimuth Display (VAD) scans – not used here. Picture from [9]

The test scans included one full 360° PPI scan and PPI scans around 304° (azimuth angle given by the lidar, i.e. relative to its own North reference) with various elevation angles. After analysis by DTU it was found out that the first elevation angle for which the laser beam was not hitting the mast was 14.1°. This was about 0.6° larger than expected, which corresponds to an error in the height difference between the lidar scanning head and the top of the mast of about 2m. This was identified to possibly be due to the presence of the lightning finial that was removed on the 7th of August.

The following test scans were run on the 19th of August by SSE in order to decide on the final elevation angle of the lidar scanning head:

- 9 PPI scans with various elevation angles between 13.3° and 14.1° (increment of 0.1°)
  Azimuth angle between 281.5° and 326.5°

  Scanning speed: 0.5°/s

  Accumulation time: 0.5s
- 10 RHI scans with various azimuth angles between 303.8° and 304.7°(increment of 0.1°)
  Elevation angle between -1.2° and 14.1°

  Scanning speed: 0.5°/s

  Accumulation time: 0.5s

Figure 13 shows a clear peak at the azimuth angle 304° for elevation angles between 13.4° and 13.8°(included) indicating that the laser beam hit the tube on which the top anemometer was mounted. For these four elevation angles, the maximum CNR was found at the lidar range 272m (including the 26m offset discovered during the calibration [1]), as shown in Figure 14, corresponding to height

between 63.0 and 64.9m above the lidar scanning head height (the inclination of the TP was not taken into account here).

At 13.3° elevation angle, high CNR values are observed for 3 azimuth positions 304°, 303.5° (2.3m to the left) and 304.25° (1.5m to the right). These maxima are observed around 270m range, corresponding to a height of 62.1m above the lidar. The most likely explanation is that the laser beam is hitting the vane and the control anemometer on each side of the mast, 2m below the top cup anemometer, although the boom length is of 3m on both sides. Nevertheless, some inaccuracy can be expected on the short horizontal distances derived from the laser beam position since the laser beam is actually continuously rotating, therefore the CNR might be averaged over a couple of meters. From 13.9° and above, the CNR remains low for all azimuth positions; the laser beam sweeps above the mast and does not hit any hard target.

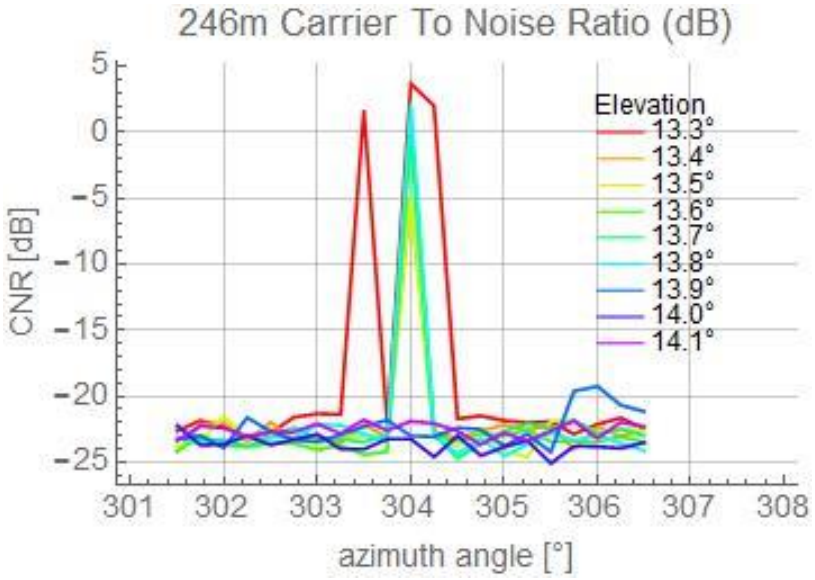

Figure 13 CNR vs azimuth angle from PPI scans with different elevation angles, at 268m range

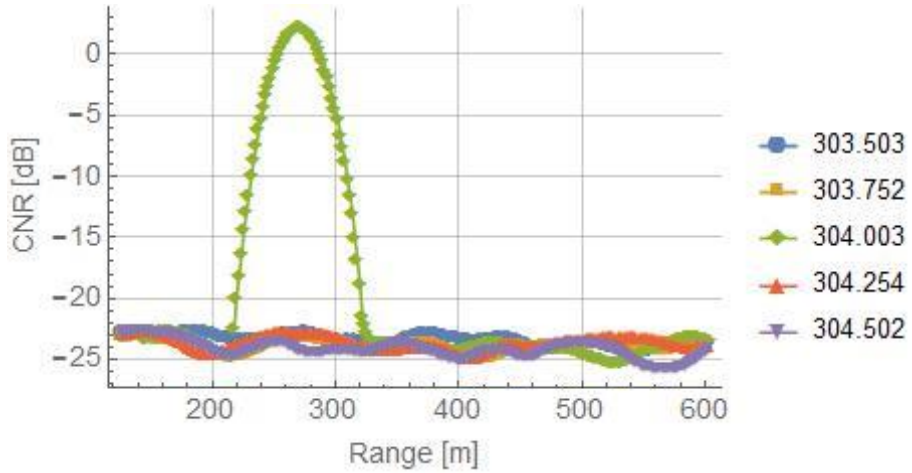

Figure 14 CNR as a function of range for various azimuth positions (shown in the legend).

From this test, we deduced that the lowest elevation angle for which the laser beam was above the mast was 13.9°; 0.5° higher than expected. The explanation for this difference is not clear.

During those scans, the wind speed was around 10.47m/s and the wind direction around 289° which probably contributed to tilt the TP platform, and therefore the lidar beam, upwards. The converted angle along the 247° direction (between lidar and mast) from the inclinometers readings is oscillating around 0.06°. The inclination of the platform was ignored in the elevation angle estimation. Since it is positive (beam slightly upwards, it would increase the difference and not reduce it).

The TP platforms of the met mast and the wind turbine are at the same height within 20cm; i.e. the cup anemometer is at 63.2m above the lidar scanning head. The two only possible explanations we can suggest are:

- either the distance between the lidar and the met mast (264.9m) and the relative height between the lidar head and the top mounted anemometer used in the angle estimation is wrong (this would question the relative coordinates of the turbine and mast). The positions of the turbine and mast given in the wind farm documentation were used for this estimation. GPS coordinates have been measured onsite at the beginning of this measurement campaign. They coincide with the documentation within 2 to 3 m. The accuracy of these measurements was too low to be used to adjust the dimensions in the calculations. The relative distance from the lidar to the mast and the relative height from the lidar head height and the top mounted anemometer should be measured with a theodolite.
- or the indicated lidar scanning head elevation angle is wrong (maybe offset). However, this had been verified during the lidar calibration at Høvøsre [6]. The indicated scanning head elevation angle corresponded to the actual angle within 0.1°. The scanning head elevation could have changed between the test in Høvsøre and the deployment at Greater Gabbard (maybe due to a chock during transportation). There has not been any similar mechanical problem due to transportation of the scanning lidar known to us. In order to verify this hypothesis, the elevation angle of the optical head should be verified one more time after the campaign. The same method as the one followed during the calibration can be used with any obstacle providing that its height is known within 10cm and the distance between the lidar and the obstacle can be measured within 10cm. PPI scans centred on the obstacle position should be performed with various elevation angles. The lowest elevation angle for which the beam is not reflected against the obstacle (no variation of the CNR with azimuth), should be compared to the elevation angle estimated from the height and the distance of the obstacle.

PPI scans were performed with an elevation angle of 13.9° from the 20th of August 2014 to the 5th of September 2014. WINDCUBE 100S data from the 22nd and 23rd of August showed that the TP platform oscillates (Figure 15) and therefore the laser beam regularly (but not constantly) hits the mast. This appears as a high CNR for the beam azimuth direction oriented towards the mast (Figure 16). A bug in the lidar signal processing identified during the calibration (appearing as stripes in the CNR and radial wind speed display due to erroneous data) can also result in high CNR for a time period (usually until rebooting). However here, the CNR value was within the expected range for the azimuth positons that were not oriented towards the mast (see the example of the next azimuth positon in Figure 17). This indicates that the high CNR is due the backscatter caused by a hard target and not the stripy mode.

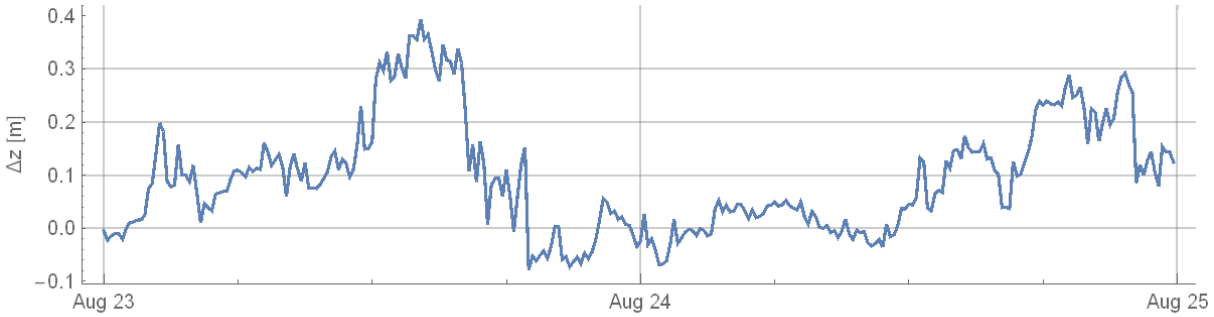

Figure 15 Deviation in lidar height beam (derived from inclinometer readings) from the default height corresponding to an elevation angle of 13.9°.

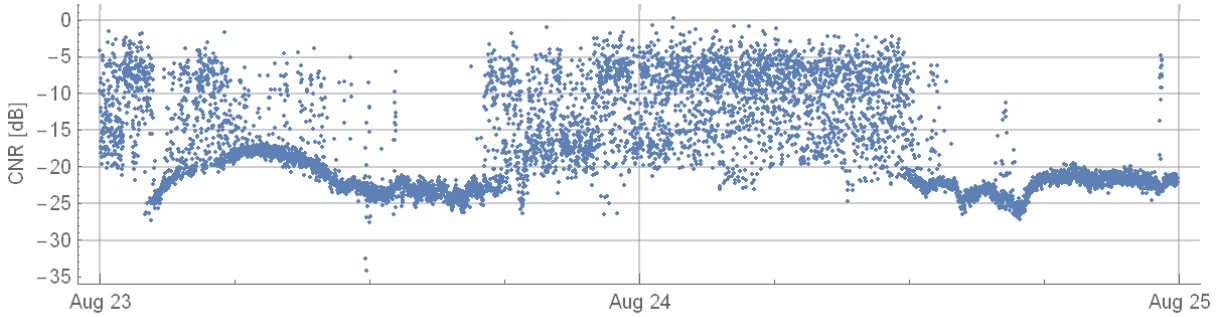

Figure 16 CNR at range 272m for the azimuth postion 305.5° (in the lidar reference)

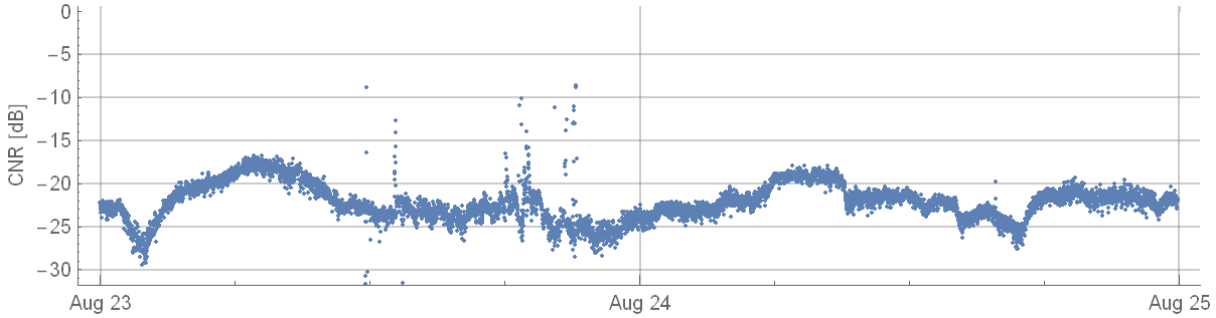

Figure 17 CNR at range 272m for the azimuth postion 302.5° (in the lidar reference)

To be on the safe side, the laser beam was raised by 0.2°, i.e. elevation angle up to 14.1°, which corresponds to an elevation by about 1m.

3.4.3 Scanning pattern

The final scanning pattern used for the measurement campaign from 05-09-2014 00:00 to 06-04-2015 00:50 was the following:

- PPI scan
- Azimuth angle between 281.5° and 326.5°
- Elevation angle: 14.1°
- Scanning speed: 3°/s
- Accumulation time: 0.5s

The lidar was configured to measure at several ranges including 272 m which corresponds to the line of sight distance between the lidar and the top of the mast with an elevation angle of 14.1°.

3.5 Wind Iris

The nacelle lidar used in this measurement campaign was a Wind Iris from Avent Lidar Technology. It is a pulsed system with 2 lines of sight separated by horizontal angle of 30° (half angle α=15°). The lidar emits a stream of pulses along each line of sight, switching between the two alternatively. This provides consecutive measurements of two radial speeds along each direction, at several distances simultaneously. The 10 minute average horizontal wind speed and direction are retrieved from the averaged radial wind speeds, based on the assumption that the wind speed is horizontally homogeneous.

3.5.1 Lidar position

The Wind Iris was placed on the nacelle of turbine IGF10 in December 2014 and the configuration was finalised on the 22nd January 2015. The optical head was mounted on the tripod, itself placed on a platform on top of the nacelle roof. At closest point, the front of the Wind Iris is 0.5 m from back of turbine blade (see Figure 18).

Figure 18 Picture of the Wind Iris on the nacelle of turbine IGF10. The front of the optical head was 0.5m behind the rotor.

The optical head was installed on the left side of the nacelle seen from the back of the nacelle (see Figure 19) as agreed upon between GGOWL and Siemens. According to the Wind Iris manual, beam 1 is on the left and beam 0 on the right when looking from behind the lidar.

Figure 19 Picture of the Wind Iris on the nacelle of turbine IGF10.

The lidar optical head was aligned with the turbine shaft. The lidar red leds were aligned to a line drawn on the nacelle roof parallel to the turbine shaft (see Figure 20).

Figure 20 Alignment of the Wind Iris optical head (using the red leads – one in the back, shown on the picture, and one in the front, not shown on this picture) to the turbine shaft (represented by a line drawn on the nacelle roof).

The Wind Iris optical head was at 2m from the center of the turbine tower (reference for turbine coordinates). The measurement range was therefore configured to be 265m, in order to measure at the same distance from the rotor as the met mast.

3.5.2 Lidar optical head pre-tilt

The Wind Iris optical head needed to be tilted downwards in order to account for the lidar height above hub height and the tilting of the turbine nacelle when the turbine is in operation, so that the beams were measuring at hub height 265m in front of the rotor [10].

The height from the centre of the main hub bearing (centre of shaft) to underside of nacelle roof was measured at 1930 mm, the roof plate is 4mm thick, and the mounting platform is 58mm high above the nacelle roof. These dimensions are given with +/-20mm tolerance on accuracy. There is 810mm between the top of mounting plate to the bottom of the Wind Iris head and the Wind Iris head is 190m high. Assuming the laser height is in the middle of Wind Iris head, the laser height from the centre of main bearing is:

1930 + 4 + 58 + 810 + 95 = 2897 mm.

The optical head needed to be pre-tilted in order to account for the height difference between Wind Iris optical height and hub height (Arctan(2.90/(267-2))), the nacelle when turbine operating at 8m/s (0.13° - from Siemens simulations) and the nacelle tilt angle at stand-still (- 0.04° - from Siemens simulations). The final indicated tilt should have been:

tilt calibration offset – pretilt=0.04-(0.63+0.13-(-0.04)) = -0.76°

However this could not be adjusted as wanted due to a large movement of the turbine nacelle (within +/-1°) during this operation (see section 7.2).

3.6 Time Synchronisation

All measurement systems (mast data loggers, SCADA, TPPI, Wind Iris and WINDCUBE 100S) were regularly synchronized – at least once a day - to the same time server as the SCADA system in order to ensure a time shift shorter than 6 seconds between the systems through the whole measurement campaign.

4. Data collection and wind conditions

Figure 21 shows the data coverage from the 23-01-2015 to the 06-04-2015 (period for which both lidars were measuring simultaneously). Every line relates to one measurement field. Colors mean presence of data while a cream background is directly connected with absence of data.

The two top lines show the availability of data from the mast data loggers and the third one from the turbine TPPI.

The following 16 lines correspond to the various signals from the Wind Iris (10 minutes statistics). Note that for this lidar (contrary to the WINDCUBE 100S) the inclinometer data are provided in the same file as all the other data). Wind speeds of 0m/s have been found in the Wind Iris data files provided by SSE. Those 0m/s events seem to be occurring when the CNR is low along one or both beams. In such a case, the horizontal wind speed cannot be reconstructed and the lidar software should return no value (“NaN” or “null”). We suspect that this is a feature of the software used in SSE to create the csv data files which has converted non numerical values into “0”. (Lidars can only return 0m/s velocity if the laser hits a hard target, on both LOS. This could not happen here.) Exceptionally, we have excluded all Wind Iris horizontal wind speed values equal to 0.0m/s, assuming they were corresponding to missing data. These periods appear as gaps in Figure 21. Overall, Wind Iris data have been missing only for very short time periods.

The remaining lines concern the WINDCUBE 100S. For this lidar, raw PPI data files were sent by SSE/GGOWL to DTU and DTU run the executable file provided by Leosphere to calculate the 10 minute statistics, including the reconstructed mean horizontal wind speed and direction as well as the “confidence factor”, CF, which gives an indication of the quality of the reconstructed values, the 10 minute availability and statistics of the CNR and spectral broadening. The last 3 lines show the availability of the data from the lidar external PTH probe.

Several holes appear in the WINDCUBE 100S data, they are generally due to technical problem of the lidar, which required rebooting or manual intervention (e.g. in November, condensation was observed on the window of the lidar scanning head; the desiccant bag was changed and the window was cleaned). Furthermore, it can be noted that the reconstructed wind speed and direction are sometimes missing whereas the other lidar channels are available. This means that the reconstruction algorithm returned a “null” usually due to low CNR or system malfunctioning (“stripy” mode).

The two lines named “Mean_Pitch” and “Mean_roll” show the data availability from these inclinometers. Those inclinometers are add-on to the device. They were functioning independently from the main data acquisition system of the lidar. The data availability for these two outputs is therefore different from the other outputs, which were all obtained with the acquisition system.

The last line shows the data coverage after applying the filters mentioned in section 6

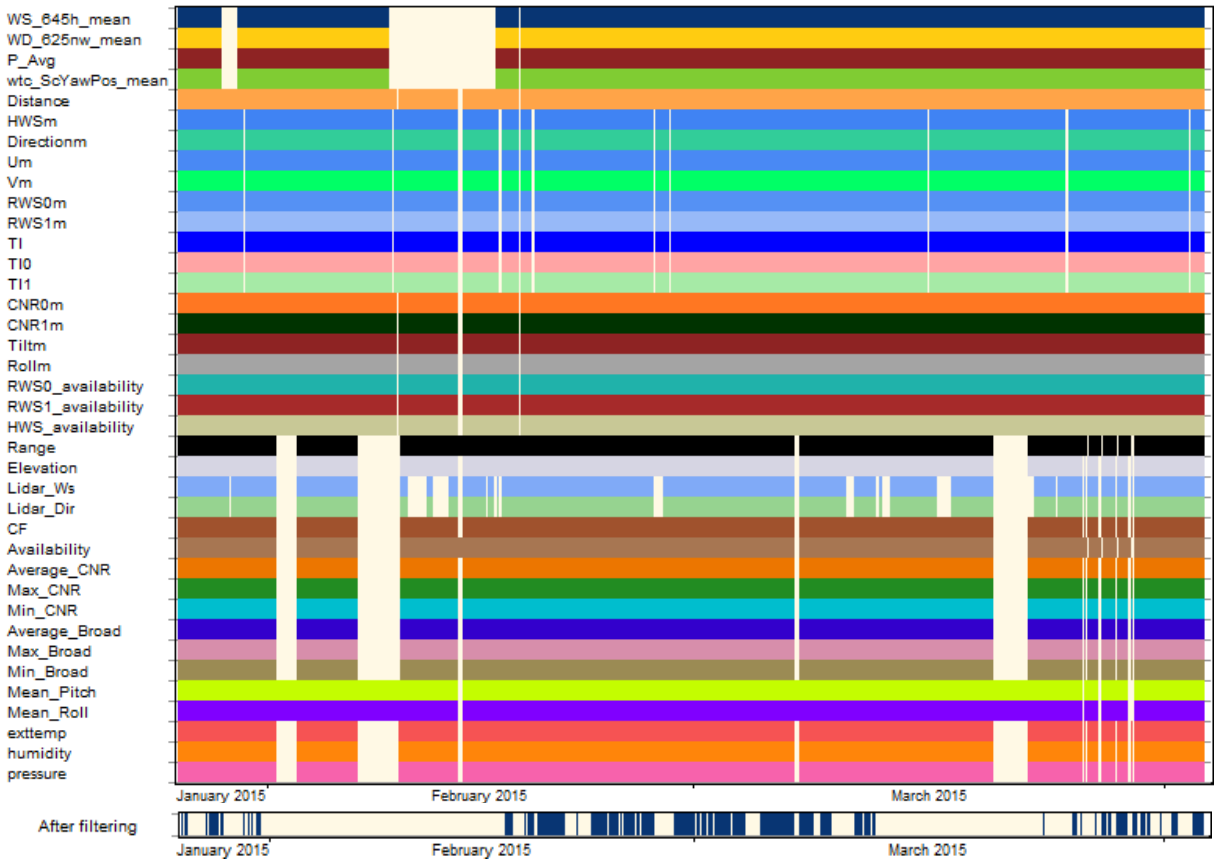

Figure 21 Data coverage

Figure 22 and Figure 23 show the wind conditions during the measurement period from 23rd of January 2015 to 6th of April 2015 (in blue) and for the power curve data set (see filters applied in section 6).

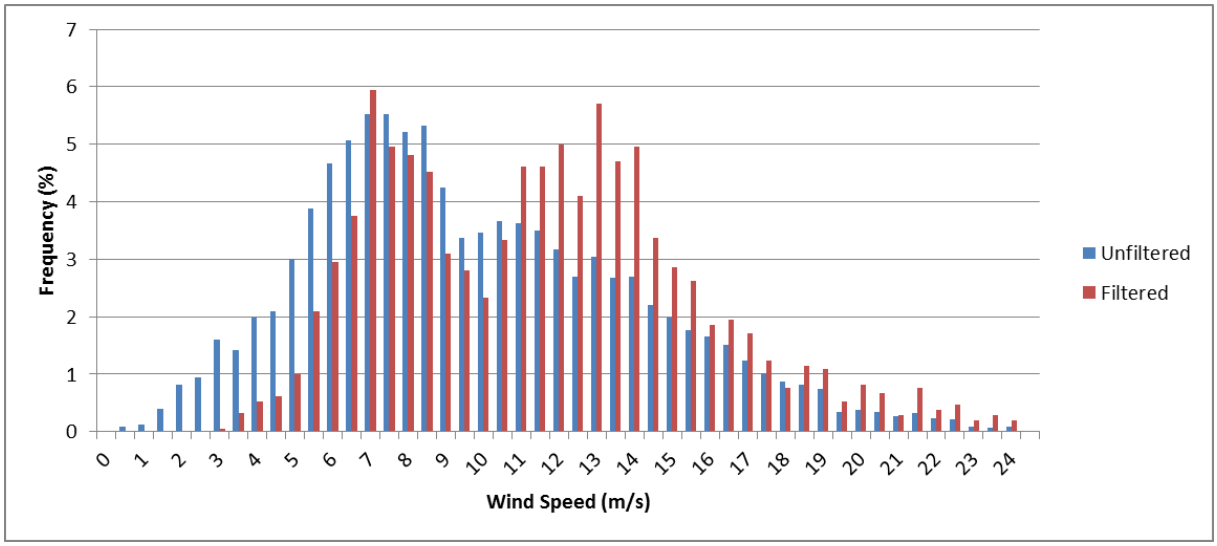

Figure 22 Mast top cup speed distribution (in percentage of total amount of data within the respective dataset) before and after filtering for power curve analysis

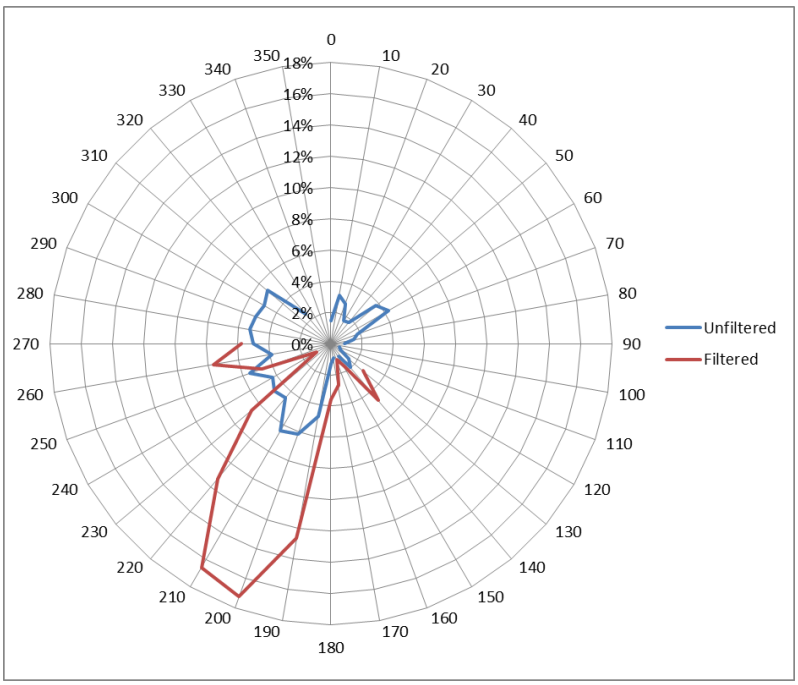

Figure 23 Wind rose from the mast wind vane at 77.5m (in percentage of total amount of data within the respective dataset) before and after filtering for power curve analysis

5. Lidars data before filtering

5.1 WINDCUBE 100S

5.1.1 Confidence factor

The “confidence factor”, CF, provides an indication of the quality of the reconstructed 10 minute wind speed and direction. According to Figure 24, there is no dependence of the CF to the wind speed. In the rest of the analysis (sections 8 to 10) the data with a CF below 0.85 have been excluded (based on the recommendations from the calibration report [1]).

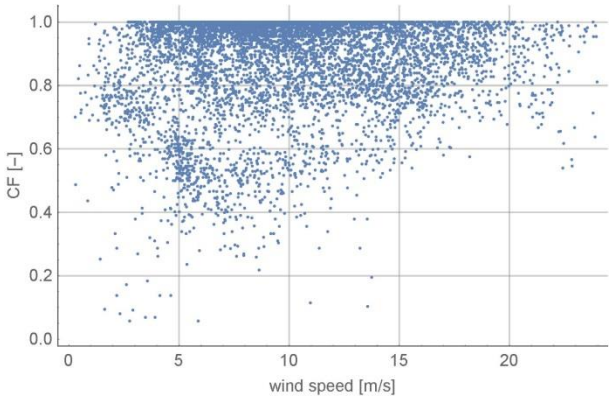

Figure 24 WINDCUBE 100S confidence factor (CF) vs wind speed

The CF on the other hand has a clear dependence on the wind direction, as shown in Figure 25. The CF decreases around 247°, direction between the turbine and the mast. A similar behavior was observed during the calibration of the WINDCUBE 100S in Høvsøre. However since we neither know the algorithm for the reconstruction of the wind speed and direction, nor the exact definition of the CF parameter, it is not possible to give a firm explanation for this behavior.

A common approach to reconstruct the horizontal wind speed and direction from a sector scanning lidar is to fit the radial wind speed measured with various azimuth angles of the lidar beam to a cosine function. Assuming this approach is used in the reconstruction algorithm of the WINDCUBE 100S, and that the CF is influenced by the goodness of this fit, the CF is expected to be low in inhomogeneous flows. For example, for wind directions below 90° and above 300°, the lidar beam is in the wake of the turbine under test or of surrounding turbines. The wind within the sector scan is very non-homogeneous; the fit of the radial wind speed to a sine function of the azimuth position is poor, which might result in a low CF value. The CF might also be low for wind directions around the centerline of the sector scan, as this corresponds to the top of the cosine function, where the fit may be more sensitive than in other parts of the cosine curve (corresponding to other wind directions).

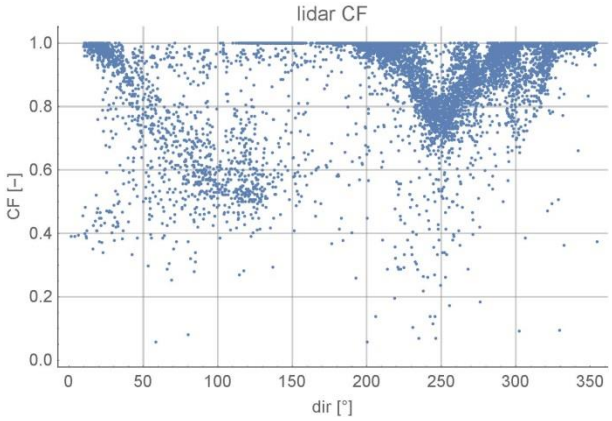

Figure 25 WINDCUBE 100S confidence factor (CF) vs wind direction

5.1.2 10 minute availability

Although the exact definition of this parameter is not known to us because it depends on the wind speed reconstruction algorithm, the 10 minute availability is expected to quantify the relative number of valid measurements obtained relative to the maximum number of measurements that can be expected within 10 minutes. We observed that the CF was not necessarily correlated to the 10 minute "availability" returned by the lidar. An example is shown in Figure 26. At 15:30 and 15:50 on the January the 9th 2015, CF is above 0.85 whereas the availability was below 70%. Those two events correspond to 10 minute period for which the mean wind speed returned by the lidar deviated from the cup anemometer wind speed by more than 2m/s. Figure 27 shows the general dependence of the wind speed deviation (difference between cup anemometer and lidar wind speed) to the availability parameter in the unfiltered dataset. The large deviations over all the range show the insufficiency of availability as the only data quality criteria. Figure 28 shows the frequency distribution of the availability parameter. Based on those figures, we have chosen to filter out the data with an availability lower than 95% for the power curve measurements analysis (see section 5).

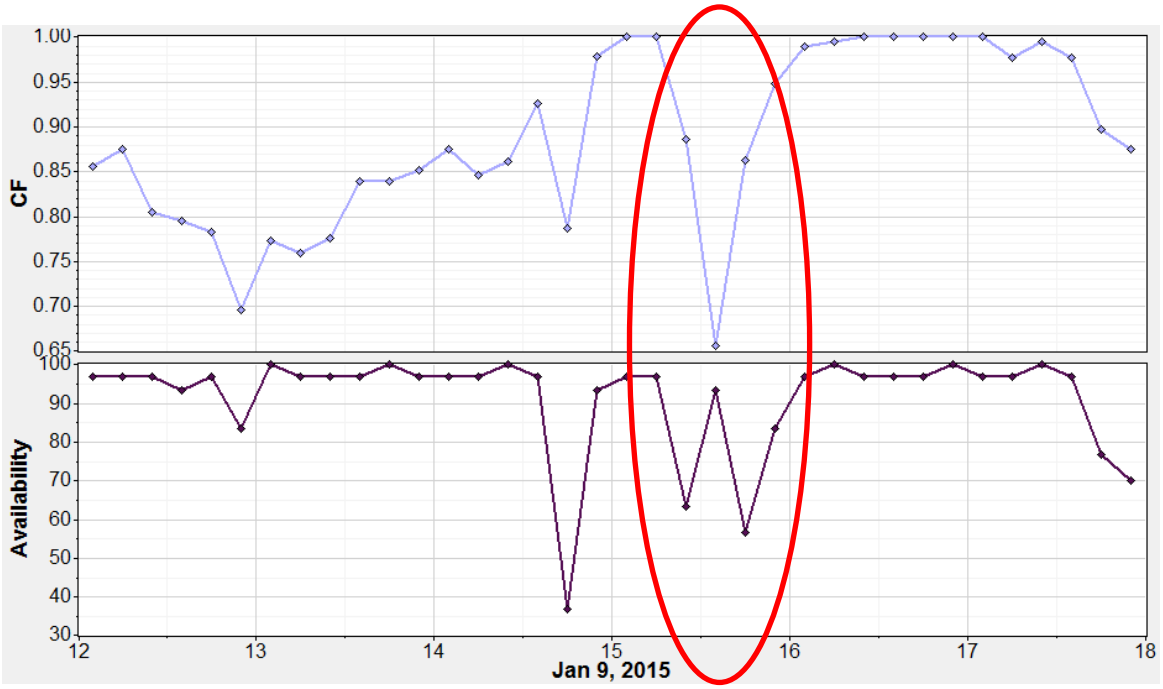

Figure 26 Simultaneous time series of CF (top) and availability (bottom) showing two events where CF>0.85 and availability <70%

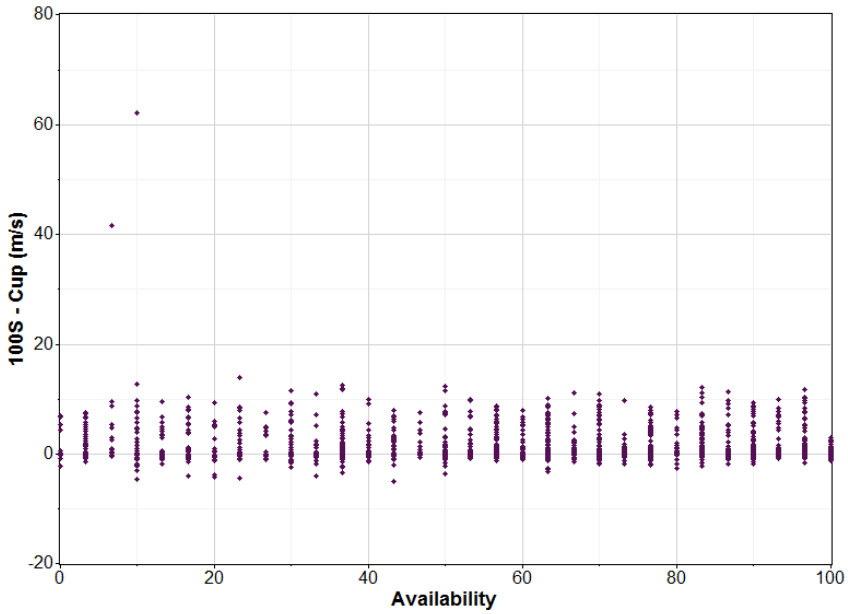

Figure 27 Lidar wind speed deviation (difference between cup anemometer and lidar horizontal wind speeds) vs WINDCUBE 100S 10 minute availability

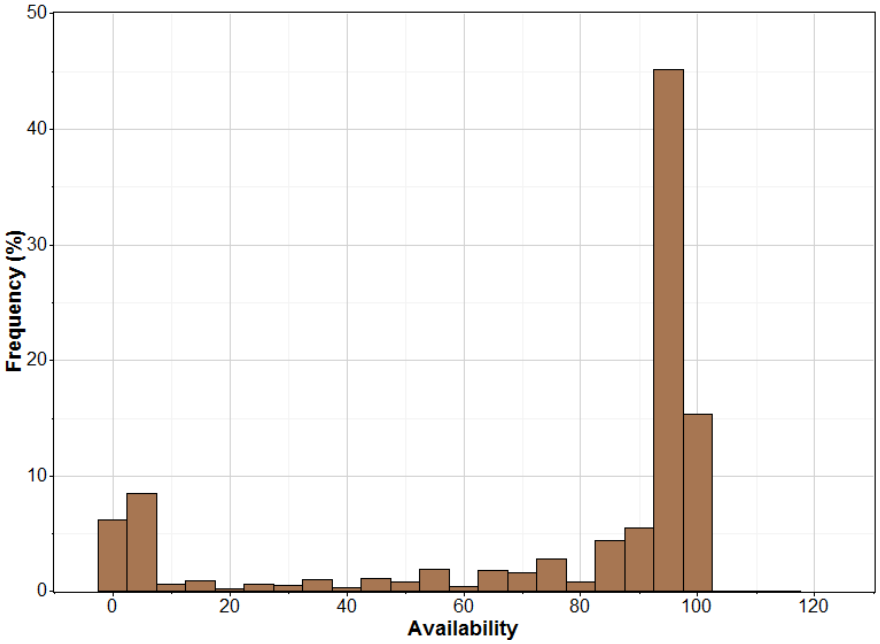

Figure 28 Frequency distribution of the WINDCUBE 100S 10 minute availability

5.2 Wind Iris

5.2.1 CNR and 10 minute availability

The CNR (Carrier to Noise Ratio) is equivalent to the Signal to Noise Ratio (SNR) and quantifies the power of the backscattered signal detected by the lidar relative to the background noise. Figure 29 shows the 10 min averaged CNR for each beam of the Wind Iris. The CNR is always lower for beam 0 than for beam 1. This systematic difference has not been observed during the calibration of the Wind Iris at Høvsøre. This is therefore probably due to the fact that beam 0 is interrupted by the rotor blades more often than beam 1, because the lidar was installed on the left side of the turbine nacelle (see Figure 10). If the lidar had been centered between the two sides of the nacelle, the CNR obtained with both beams would very similar.

On several occurrences however, the CNR of both beams has been very low (below -25dB). Such events could be due to a blade stopped in front of the optical head. Since it was placed very close to the rotor, one blade may have intercepted both beams simultaneously. Another possible explanation is a significant change in the aerosols distributions, like fog for example. If a thick fog cloud stands in front of the lidar, the CNR from the close ranges will be higher than usual, but as the laser beam cannot propagate further, very weak signals will be detected for longer ranges and the CNR from those ranges will be very low. When the CNR is very low, the Wind Iris lidar does normally not return any wind speed value. Those events correspond to the 0.0 m/s events mentioned in section 4, they were therefore artificially removed before proceeding to any further analysis.

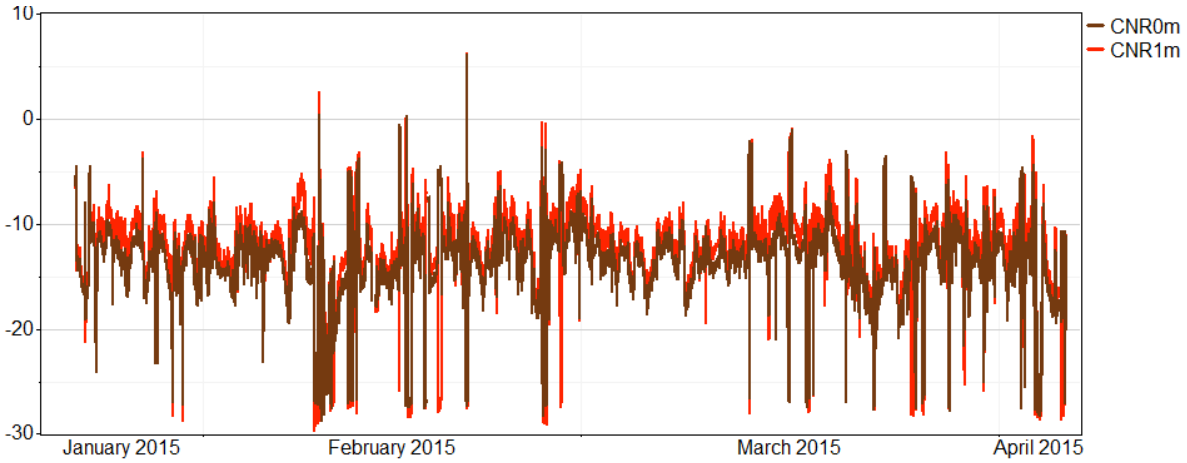

Figure 29 Time series of the Wind Iris CNR for both beams for the range 265m

Figure 30 and Figure 31 show the 10 minute availability of each beam as a function of the horizontal wind speed. The 10 minute availability of each beam is defined as the ratio between the number of valid radial wind speeds recorded for this line of sight and the number of stream of pulses emitted along this line of sight (in theory equal to the expected number of radial wind speed if the CNR was constant and high enough) within 10 minutes. An availability below 1.0 is due to occurrences of low CNR (below a threshold pre-defined by the lidar manufacturer) in which case no radial wind speed is returned by the device and therefore no horizontal wind velocity is returned either (the instantaneous horizontal wind speed is reconstructed from two consecutive radial wind speed measurements, each one taken along one of the line of sight).

The availability is most of the time below 1.0 for both beams because they are partially blocked by the rotor blades passing in front of the optical head. Moreover the availability of beam 0 is lower on average than that of beam 1. This is most probably due to the fact that the lidar is not centered between the sides of the nacelle and beam 0 (the right beam when standing behind the optical head) is blocked by the blades more often than beam 1 (left beam).

The events where the availability of one or both beams was equal to 1.0 correspond to periods when the turbine status signal “generator running” was down to 0. It is therefore likely that the rotor was stopped in a position such that one or both beams were getting through the rotor continuously for the whole 10 minute period. This also corresponds to high CNR values (see Figure 32).

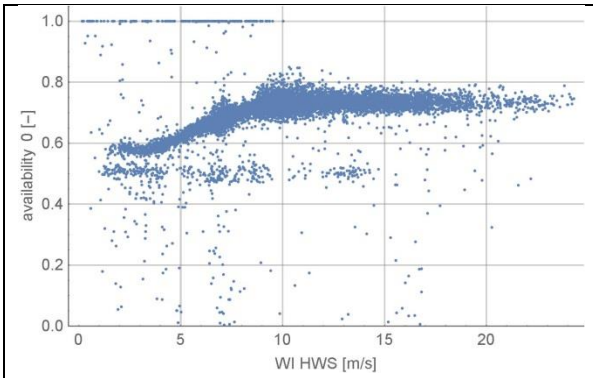

Figure 30 availability RWS0 vs horizontal wind speed from Wind Iris

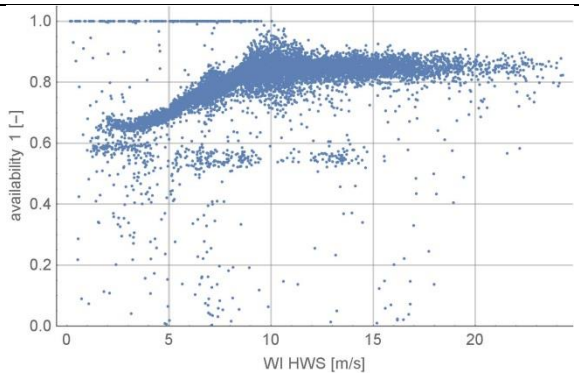

Figure 31 availability RWS1 vs wind speed horizontal wind speed from Wind Iris

The low availability values are correlated to low CNR (Figure 32). Low CNR can either occur because of one blade blocking the laser beam, in which case no signal is detected from the measurement range (here 265m) far behind the blade, or in case of high aerosol density such as fog in the first range gates. There was no clear correlation between the turbine status signals and the low CNR events, which let us think that both cases may have happened.

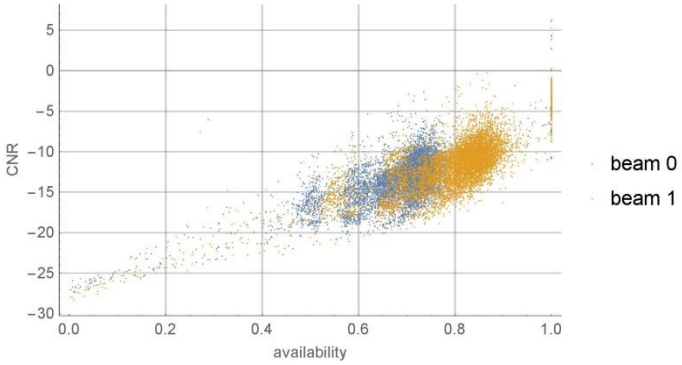

Figure 32 CNR vs availability for each beam (Blue: beam 0; Yellow: beam 1)

5.2.2 Wake of neighboring turbines

Figure 33 and Figure 34 show the 10 minute mean lidar wind speed deviation, i.e. difference between the Wind Iris horizontal wind speed and the cup anemometer wind speed. The large positive deviations are occurring for specific wind directions as shown in Figure 34.

For wind directions around 67°, the Wind Iris is measuring the wind speed ahead of IGF10 (in single wake of IGG11) while the mast is in the double wake of IGF10 and IGG11 (between 48° and 86°) and therefore measuring lower wind speeds than the lidar. The mast is in the wake of IGE14 between 287° and 333° whereas the lidar is disturbed by the wake of IGE14 for the sector 270° to 320° (according to the IEC formula adapted to the nacelle lidar as explained in [11]). As the disturbance on the two instruments is not homogeneous within those sectors, it appears that the lidar estimates lower wind speeds than the cup anemometer between 270° and 300° and higher wind speeds than the cup anemometer between 300° and 333°. A similar effect is observed in the wake of IGE13, the mast is in the wake of this turbine for wind directions between 342° and 18° while the lidar measurements are disturbed between 330° and 10°.

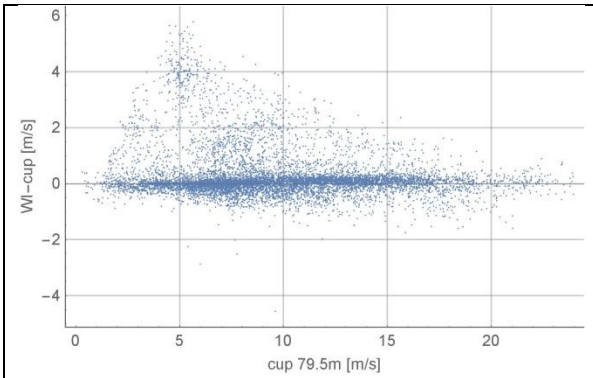

Figure 33 Wind iris wind speed deviation vs wind speed (top mas cup anemometer)

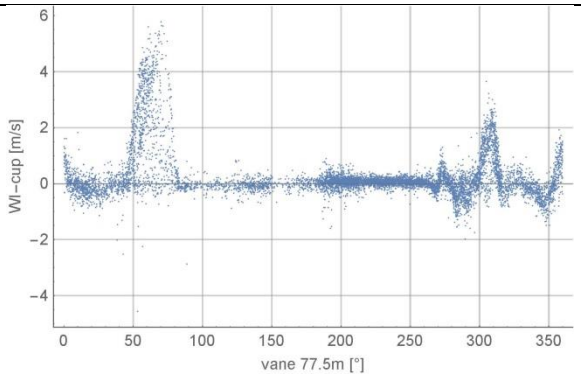

Figure 34 Wind iris deviation vs wind direction (vane)

5.2.3 Wind Iris relative direction measurement

The Wind Iris provides the reconstructed wind direction relative to the lidar axis. As the lidar has been carefully aligned with the axis of the nacelle (within 3°) this angle corresponds to the turbine yaw misalignment to the wind direction, when both lidar beams are measuring in a homogeneous inflow. However, when one of the beams is in the wake of a neighboring obstacle whereas the other beam is outside the wake, the homogeneity assumption is violated and the reconstructed relative wind direction is wrong. In Figure 35, the lidar returns a large positive angle when one beam is in the wake of the IGE14 between 270° and 285°, while it returns a large negative angle when the first beam is outside the wake and the second beam inside, between 285° and 300°. Similar patterns are observed for the wakes of IGG11 and IGE13. Those values do not correspond to real turbine yaw errors but they are artefacts of the lidar reconstruction algorithm assuming homogeneous flow.

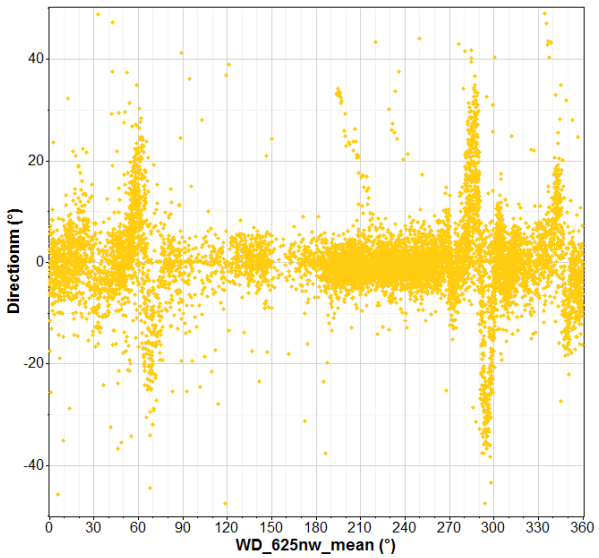

Figure 35 Relative wind direction returned by the Wind Iris as a function of the wind direction measured by the vane on the mast

6. Data filtering

For the rest of the analysis, focusing on the power curve measurement, the following filters were applied:

1) Wind direction sector: Only data with wind direction between 128° and 270° were selected. The IEC sector (used for a certified power curve based only on the met mast measurement) is 86° to 274°. However for wind direction below 128°, the WINDCUBE 100S scanning trajectory is in the wake (as defined by the IEC 61400-12-1) of the turbine under test. Above 270°, one of the beams of the Wind Iris is in the wake of turbine IGE14. The restricted sector 128°-270° was selected to ensure that neither the mast nor the scanning trajectory of the WINDCUBE 100S, nor the beams of the Wind Iris were affected by the wakes of the turbine under test or surrounding turbines.

2) Wind turbine in normal operation: the following filters were applied based on the information provided by SSE.

   - NumSamplesInterval == 600
   - NumSamplesPT == 600
   - K3 == 100 (control signal generator running)
   - K4 == 100 (control signal turbine OK)
   - K5 == 0 (Control signal power reduced)

3) WINDCUBE 100S data quality:

   a. according the recommendations from the calibration report [6], only lidar data with CF larger than 0.85 were selected;

   b. in addition to the filter on CF, we found it was necessary to apply a filter on the 10 minute availability; data with an availability lower than 95% were excluded (see section 5.1.2).

4) Wind Iris data quality: based on Figure 30 and Figure 31, we have chosen to exclude data with availability below 0.55 for beam 0 and 0.6 for beam 1.

After filtering the dataset counted 2101 data points (equivalent to about 350 hours).
The rest of the analysis (sections 8 to 10) was performed on the filtered dataset.

7. Measurement height

7.1 WINDCUBE 100S

The height of the beam was estimated by considering the beam position in the middle of the sector scan, including the scanner head elevation angle (14.1° - although we are aware this value is resulting in a larger measurement height than we believe – see section 3.4.2) and 10 minute averages of the inclinometer readings converted into a height deviation as the result of two rotations, one around the lidar North direction (Y-angle) and one around the orthogonal direction (X-angle).

Figure 36 shows the variations of the laser beam height above CD. The height of the beam clearly depends on the wind direction and wind speed. When the wind blows along a direction around 247°, the turbine tower bends backwards therefore tilting the TP platform so that the lidar beam is moved upwards. On the contrary, when the wind direction blows along a direction around 67°, the turbine tower bends in the opposite direction, tilting the TP platform so that the lidar beam is moved downwards. The bending moment, and therefore the tilting magnitude, increases as the wind speed gets closer to rated wind speed.

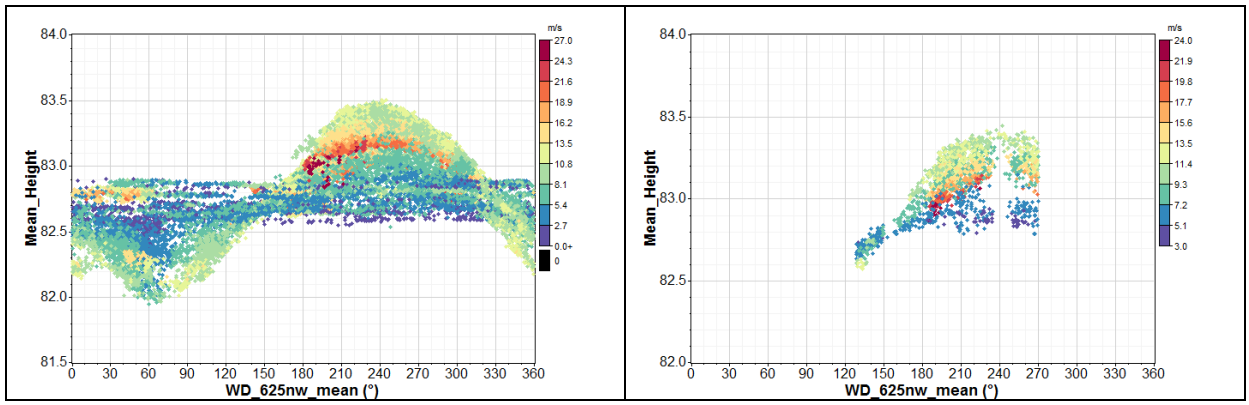

Figure 36 Ten minute average laser beam height in function of wind direction color-coded as a function of wind speed (left: before filtering; right: after filtering)

Figure 37 shows the average beam height dependency on the wind speed, within the sector used for the power curve analysis (128°-274°). The lidar was measuring between 3.55m and 3.95m above hub height (79.5m) when the lidar beam height is estimated with the scanner head elevation angle 14.1°. This is well in excess of the requirements of the IEC 61400-12-1 to measure at hub height +/-2.5%. Nevertheless, as explained in section 3.4.2, the lidar beam is expected to be only about 2m above the cup anemometer (according to the test scans with various elevation angles). If there had been no mast risking disturbing the lidar measurement, the elevation angle would have been adjusted to measure at hub height, with a variation within +/-1m (depending on the wind speed and direction).

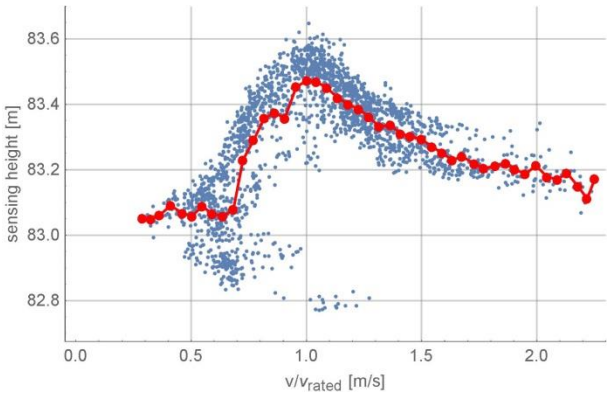

Figure 37 Lidar beam height (10 min average) vs wind speed. Red dots show the average values per wind speed bin of 0.5m/s.

7.2 Wind Iris

The tilt angle has been varying between -0.5° and 0.21° (Figure 38) while we would have liked to have it centered around -0.76° (for 8m/s) in order to have the beams at hub height 267m (mast position) ahead of the turbine rotor and for 8m/s. Similarly the roll angle should have been centered around +0.38° (offset measured during the inclinometer calibration [5]) but has been measured between -0.25° and +0.3° (Figure 40). Adjusting the tilt and roll has been very challenging because the turbine nacelle was tilting within +/-1.0° although the turbine was stopped and the wind speed rather low during this operation. This may be due to the offshore conditions, where the turbine is also affected by the wakes and currents, and maybe the monopile foundation that enhances the turbine nacelle motion. The tilt standard deviation (Figure 39) is about twice larger than what was observed in Avedøre, Denmark, where a Wind Iris was installed on an offshore wind turbine but in shallow water, only a couple of meters from the coast [11]. Perhaps, using an averaged value of the tilt and roll over a period of time (e.g. 1 min) instead of the instantaneous angles, during the adjustment of the optical head inclination would reduce the influence of the turbine nacelle motion.

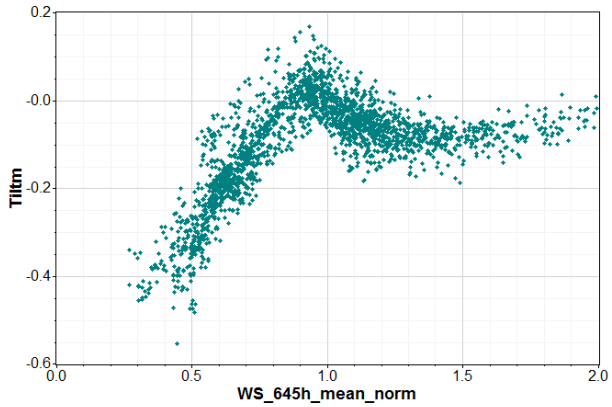

Figure 38 scatter plot of the 10 min mean lidar tilt vs wind speed

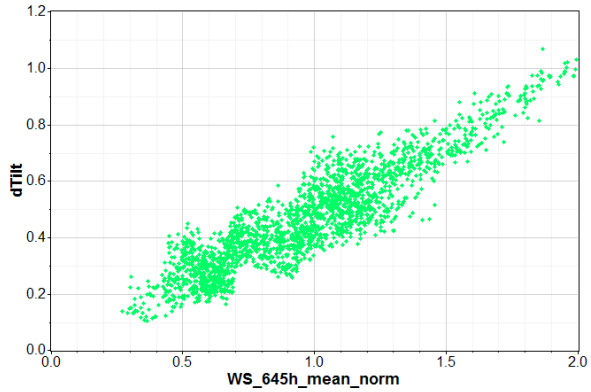

Figure 39 scatter plot of the 10 min standard deviation of the lidar tilt vs wind speed

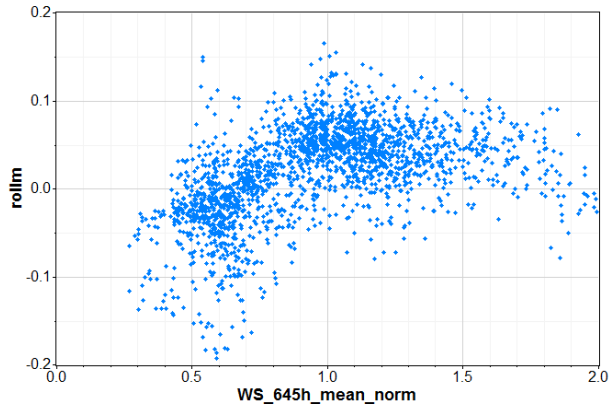

Figure 40 scatter plot of the 10 min mean lidar roll vs wind speed

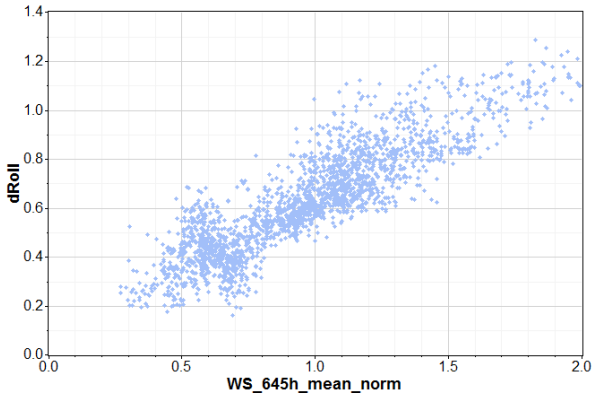

Figure 41 scatter plot of the 10 min standard deviation of the lidar roll vs wind speed

Figure 42 shows the average beam height dependency on the wind speed, within the sector used for the power curve analysis (128°-270°). For comparison purposes it is shown together with the beam height of the WINDCUBE 100S. The Wind Iris was measuring between 1m and 3m above hub height; this corresponds to 1.3% to 3.8% of hub height, which exceeds the requirements of the IEC 61400-12-1 to measure at hub height +/-2.5%. If we had managed to pre-incline the optical head by 0.76°, the

beam would have been within the required range. It would however not be within the range +/-1% of hub height advised in the revised version of the IEC 61400-12-1. The deviation in measurement height could translate into a large wind speed deviation in case of large wind shear. However, the wind shear was relatively low for this data set (as shown in Figure 43). The shear exponent was estimated with the wind speeds measured with the boom mounted cup anemometer at 60m and 77.5 above CD, assuming a power law profile. Nevertheless, if no met mast was available and therefore the frequency distribution of the shear exponent was unknown during the measurement campaign, this would have to be taken into account in the uncertainty estimate (see section 10).

As explained above the beam height of the Wind Iris should have been lower to be within the IEC requirement for wind speed measurement height. In the end the Wind Iris beam height was expected to be lower than the WINCUBE 100S height in this campaign because the Wind Iris should have been set up to measure at hub height, while the WINDCUBE 100S was set up to measure above the mast (in order to avoid hard target hitting while scanning). Nevertheless, if the WINDCUBE 100S was used without hub height met mast, the scanning head elevation angle would have simply been adjusted based on the wanted distance upstream and the turbine hub height above the lidar. Both lidars would have measured around the same height.

It can be clearly seen from Figure 42 that the range of variations in the beam height is smaller for the WINDCUBE 100S installed on the TP than for the Wind Iris mounted on the turbine nacelle. The TP platform moves less than the nacelle.

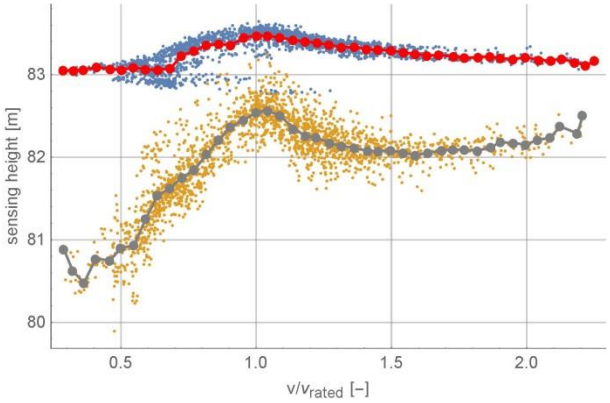

Figure 42 Lidar beam height (10 min average) vs wind direction. Red dots show the average values per wind speed bin of 0.5m/s.

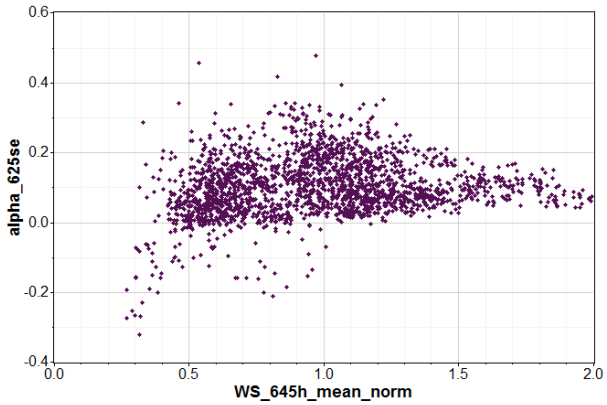

Figure 43 Shear from mast vs top cup wind speed (normalized)

8. Comparison of lidars measurements to mast measurements

8.1 Wind speed

8.1.1 WINDCUBE 100S

The reconstructed 10 minute mean wind speed from the WINDCUBE 100S compares fairly well to the measurements from the mast top mounted cup anemometer, as shown in Figure 44. The regression line equation indicates that the lidar measures a slightly higher wind speed than the cup anemometer (0.23% at 10m/s).

This result is slightly different from the calibration result where the linear regression between the WINDCUBE 100S horizontal wind speed and the reference cup anemometer corresponded to a slight underestimation by 0.07% at 10m/s. This difference may be due to the different cup anemometer types used at the two sites (Wind Sensor at Greater Gabbard and Thies First Class at Høvsøre) and to the different external conditions, especially air temperature and turbulence intensity which influence the response of the cup anemometers.

Note that it has been chosen here not to apply the calibration results as a correction to the lidar wind speed measurements taken offshore, because the deviation between the lidar and reference cup anemometer wind speed during the calibration was very small compared to the reference uncertainty [6]. Correcting the lidar wind speed measurements based on this calibration result would only make a very minor difference in the power curve results.

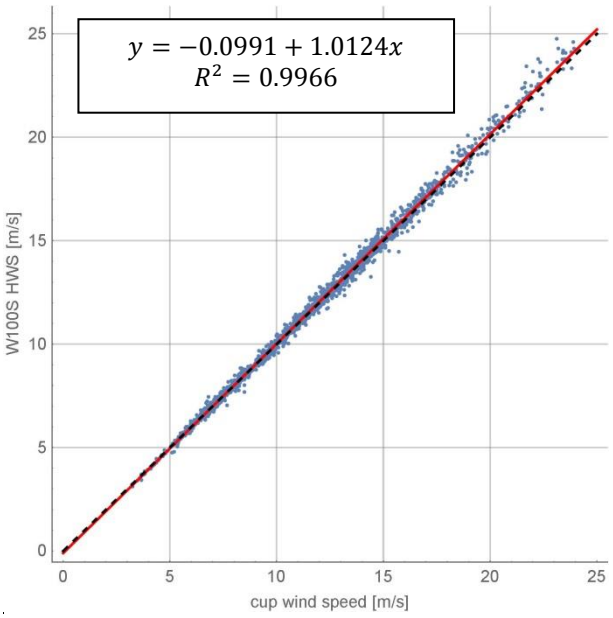

Figure 44 Scatterplot of W100S wind speed versus cup

Figure 45 and Figure 46 give a closer look into the deviation between the WINDCUBE 100S horizontal wind speed and the mast top mounted cup anemometer wind speed. The scatter increases with the wind speed (Figure 45). The observation of the dependence of the deviation on the wind direction (Figure 46) is affected by the filtering on the CF which has removed most of the data within 247°+/-30° (see subsection 5.1.1).

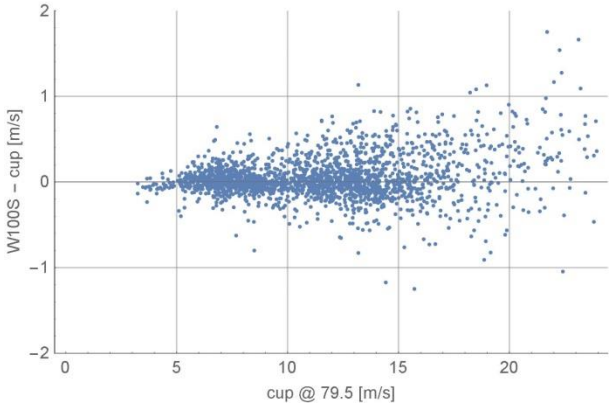

Figure 45 Wind speed deviation vs. wind speed

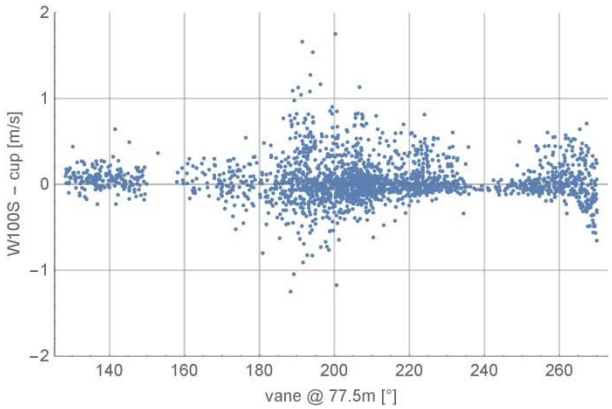

Figure 46 Wind speed deviation vs. wind direction

8.1.2 Wind Iris

The reconstructed 10 minute wind speeds from the Wind Iris are in good agreement with the measurements from the mast top mounted cup anemometer, as shown in Figure 47. The regression line equation indicates that the lidar measures a slightly higher wind speed than the cup anemometer (0.36% at 10m/s). Similarly to the WINDCUBE 100S case, it has been chosen not to apply the calibration results as a correction to the lidar wind speed measurements taken offshore, because the deviation between the lidar and reference cup anemometer wind speed during the calibration was very small [5].

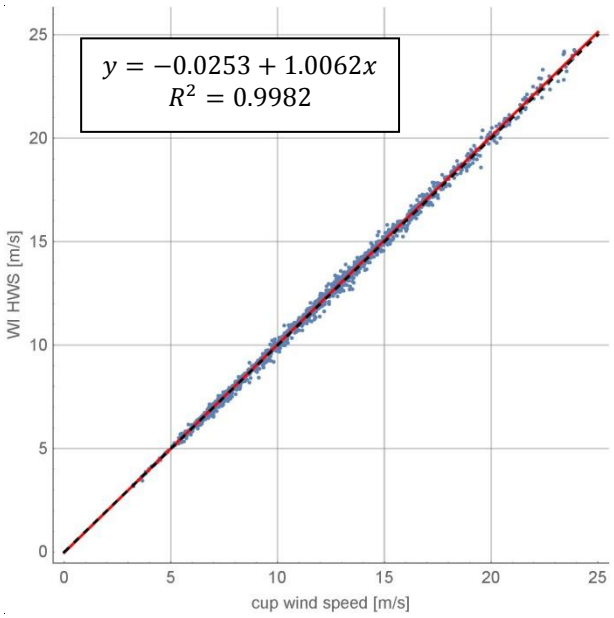

Figure 47 Scatterplot of Wind Iris wind speed versus cup

Figure 48 and Figure 49 show the deviation between the Wind Iris horizontal wind speed and the mast top mounted cup anemometer wind speed for the filtered dataset. The deviation slightly increases with the wind speed (Figure 48).

The scatter is varying with the wind direction (Figure 49). The missing data around 247° are due to the filter applied on the WINDCUBE 100S CF factor (this is a common dataset to both lidars). A possible explanation for the increase in scatter around 270° is that the Wind Iris beams are in the wake of turbine IGD13 for wind directions around between 260° and 288°. This has not been removed when choosing the wind sector according to the procedure described in [10], which is based on the IEC 61400-12-1, because in this procedure only the wakes from wind turbines up to 20D from the turbine under test are considered, whereas IGD13 is at about 23D from the mast and 25D from the lidar measurement range. Perhaps the effect of wakes requires longer distance to decrease in offshore conditions (due to a lower roughness). Figure 50 shows the sector to be excluded for turbine IGF10 due to all surrounding turbines up to 30D distance.

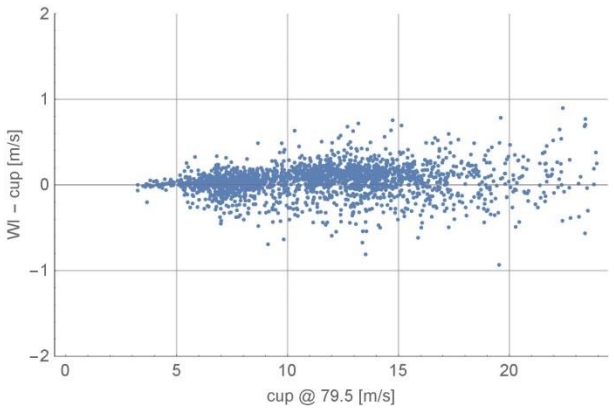

Figure 48 Wind speed deviation vs. wind speed

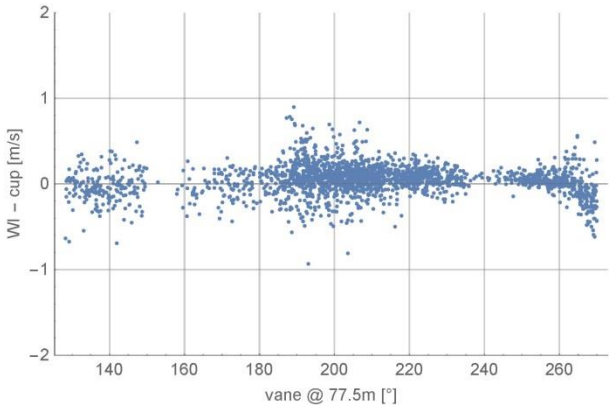

Figure 49 Wind Iris wind speed deviation vs. wind direction

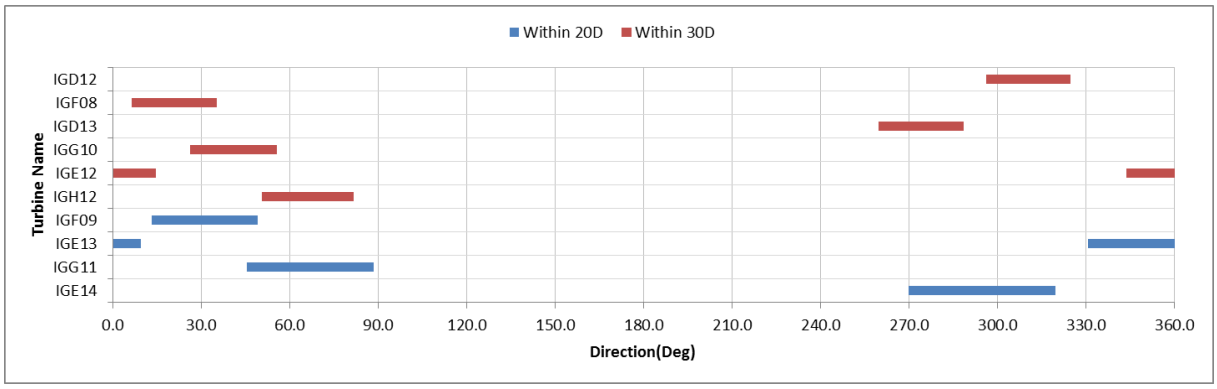

Figure 50 Width of sectors to exclude when the turbine IGF10 is in the wake of surrounding turbines

8.2 Wind direction

8.2.1 WINDCUBE 100S

The reconstructed 10 minute average wind direction from the WINDCUBE 100S also compares fairly well to the vane measurements at 77.5 m on the mast. The linear regression shows a gain error about 2.1% and an offset of about 12°. This could be due to the combination of several causes:

- The alignment of the vane which is usually within 3°;
- The offset measured between the lidar north reference and the true north, generally within 3°;
- The effect of the data distribution on the least-square regression line;
- The uncertainty in the reconstruction algorithm.

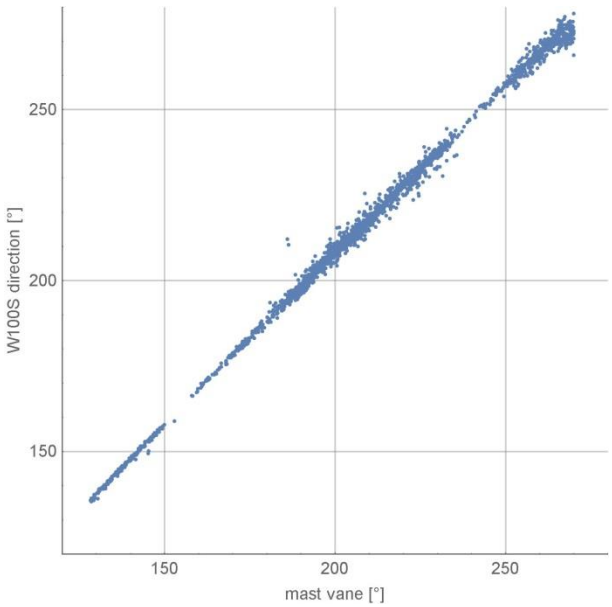

Figure 51 Scatterplot of 100S wind direction versus vane

8.2.2 Wind Iris

Figure 52 shows the relative wind direction given by the lidar as a function of wind direction after filtering. Most data are within +/-10°.

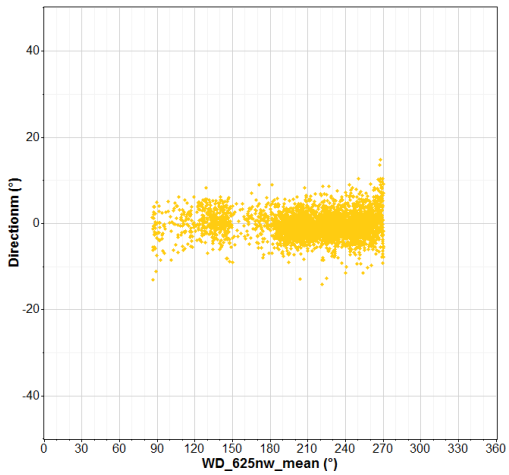

Figure 52 Relative wind direction returned by the Wind Iris as a function of the wind direction measured by the vane on the mast

8.3 Turbulence intensity

8.3.1 WINDCUBE 100S

The executable file provided by Leophere to post-process the data time series into reconstructed 10 minute statistics did not return the wind speed standard deviation. It was therefore not possible to observe the turbulence intensity measured with the WINDCUBE 100S.

8.3.2 Wind Iris

With a two horizontal forward facing beam nacelle lidar, it was observed that it was accurate and robust to use the lidar beams individually in order to retrieve turbulence intensity (TI), by computing turbulence intensity TI_0 and TI_1 on beams 0 and 1. Turbulence intensity on each beam is defined as the standard deviation dV_i of each beam's wind speed (i=0 or 1) divided by the average beam wind speed:

$$TI_i = \frac{dV_i}{\langle V_i \rangle}$$

With:

$$dV_i = \sqrt{\langle V_i^2 \rangle - \langle V_i \rangle^2}$$

TI_{lidar} is then defined as:

$$TI_{lidar} = \frac{TI_0 + TI_1}{2}$$

Figure 53 shows the comparison between the turbulence intensity measured by the Wind Iris and the cup anemometer. It has been demonstrated that the turbulence intensity measured by a lidar depends on the atmospheric stability [12, 13, 14], which generally appears as a large scatter, since the lidar either underestimates the TI (under stable conditions) or overestimates the cup TI (under unstable conditions).

However here an offset can be observed, the lidar generally returns a smaller TI than the cup anemometer. Further analysis would be required on the data time series to investigate whether this could be due to the difference in availability between the two beams caused by the position of the lidar on the side of the nacelle (it might be resulting in different radial wind speed turbulence intensity); and/or to the large tilting movement of the turbine that might influence the radial wind speed turbulence intensity as well.

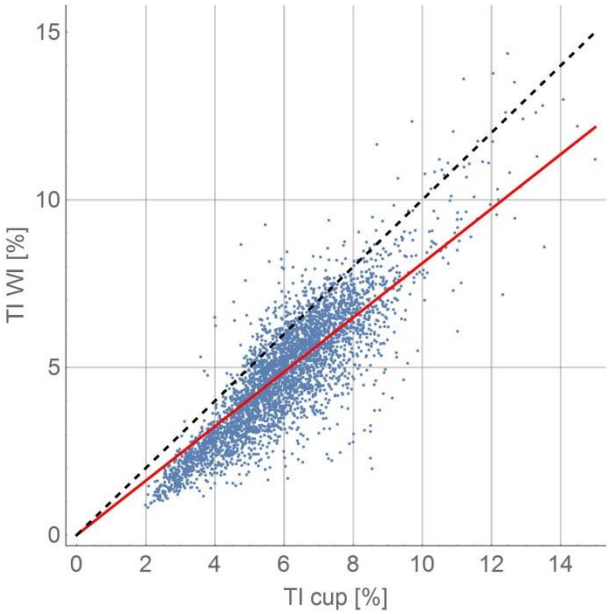

Figure 53 Turbulence intensity from the Wind Iris vs turbulence intensity from the cup anemometer (Dashed black line: 1:1 line; Red line:least square linear regression forced through the origin:y=0.816x, R^2=0.964)

9. Power curve and AEP

9.1 Power curve

Figure 54 to Figure 56 show the power curve scatter plot obtained with the mast top cup anemometer, the WINDCUBE 100S and the Wind Iris respectively, using a concurrent dataset for all three instruments (i.e. the exact same filtering was applied – see section 6). The scatter is a little larger for the WINDCUBE 100S (Figure 55); this is the consequence of the scatter observed in Figure 45. On the other hand the scatter is slightly smaller for the Wind Iris (Figure 56). This is probably due to the fact the nacelle lidar is always measuring upwind. The correlation between the wind speed measured upstream by the lidar and the turbine power is larger than the correlation between the wind speed measured by the cup anemometer and the turbine power because the met mast has a fixed position, and can for some wind directions be on the side of the wind turbine [1]. Nevertheless since the wind speeds compared well on average, the bin-averaged power curves are very similar to each other. Figure 57 shows the measured power curve obtained with each instrument, after applying the method of bin form the IEC 61400-12-1 (data binned in wind speed bins of 0.5m/s centered on factors of 0.5m/s).

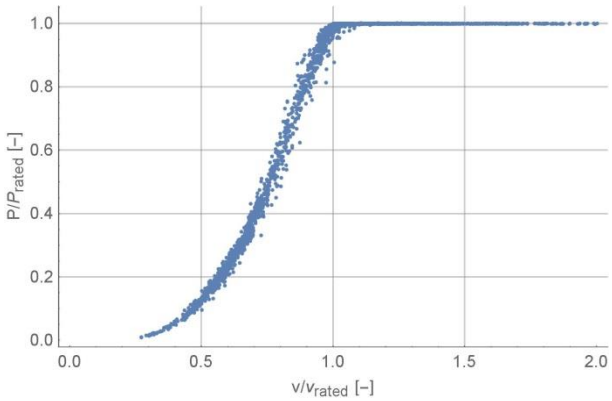

Figure 54 Power curve scatterplot – cup anemometer

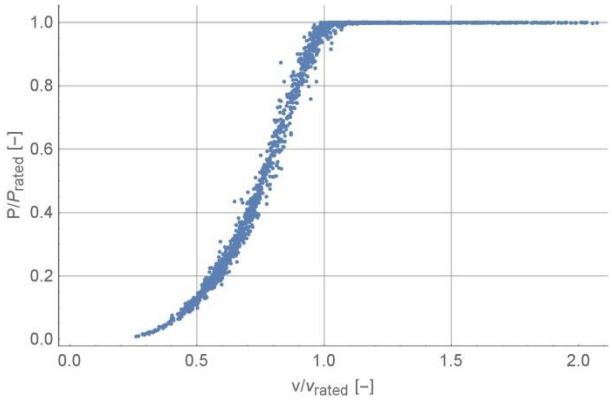

Figure 55 Power curve scatterplot - WINDCUBE 100S

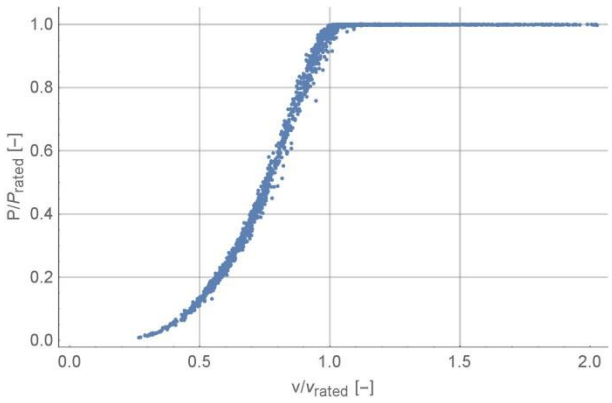

Figure 56 Power curve scatterplot - Wind Iris

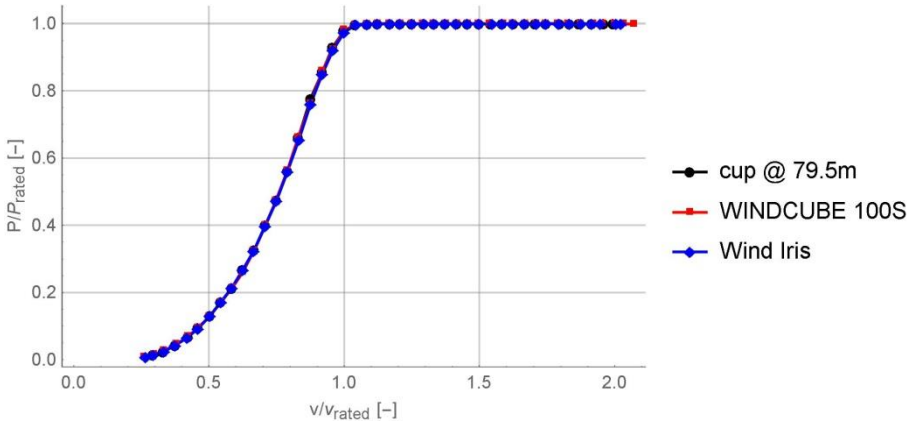

Figure 57 Bin averaged power curve for both instruments

9.2 AEP comparison

The extrapolated AEP was calculated for annual average wind speeds between 4 and 11m/s for the previous power curves, see Table 3. The AEP obtained with each lidar is given relatively to the cup anemometer AEP. When the lidars measure a higher wind speed than the cup anemometer, the power curve is underestimated (i.e. shifted towards high wind speed) and the lidar derived AEP is lower than the cup anemometer derived AEP. While when the lidar measure lower wind speed the opposite happens in terms of AEP.

Table 3 Extrapolated AEP for the cup anemometer power curve and the 2 lidar power curves

Hub height annual average wind speed	WINDCUBE 100S AEP relative to cup AEP	Wind Iris AEP relative to cup AEP
m/s	[%]	[%]
4.0	100.76%	99.71%
5.0	100.11%	99.60%
6.0	99.92%	99.57%
7.0	99.87%	99.60%
8.0	99.86%	99.68%
9.0	99.87%	99.82%
10.0	99.88%	100.03%
11.0	99.89%	100.30%

10. Uncertainty

The total power curve uncertainty results from the combination of the category A uncertainty in power and the category B uncertainty in wind speed, in temperature and in pressure. In this analysis, the lidar wind speed and the cup anemometer wind speed were corrected for air density using the temperature and pressure measurements from the met mast. Therefore the expected differences in uncertainty between the two power curves are the category A uncertainty and the category B uncertainty in wind speed.

10.1 Category A uncertainty

The category A uncertainty in power is defined as the standard deviation of the power divided by the square root of the number of data points in the bin [3]. As shown in Figure 58, the category A uncertainty obtained with the WINDCUBE 100S is slightly larger than that obtained with the mast top mounted cup anemometer, because of the larger scatter discussed above (subsection 9.1). On the other hand the lower scatter observed in the power curve scatter plot obtained with the Wind Iris (Figure 56) results in a slightly lower category A uncertainty.

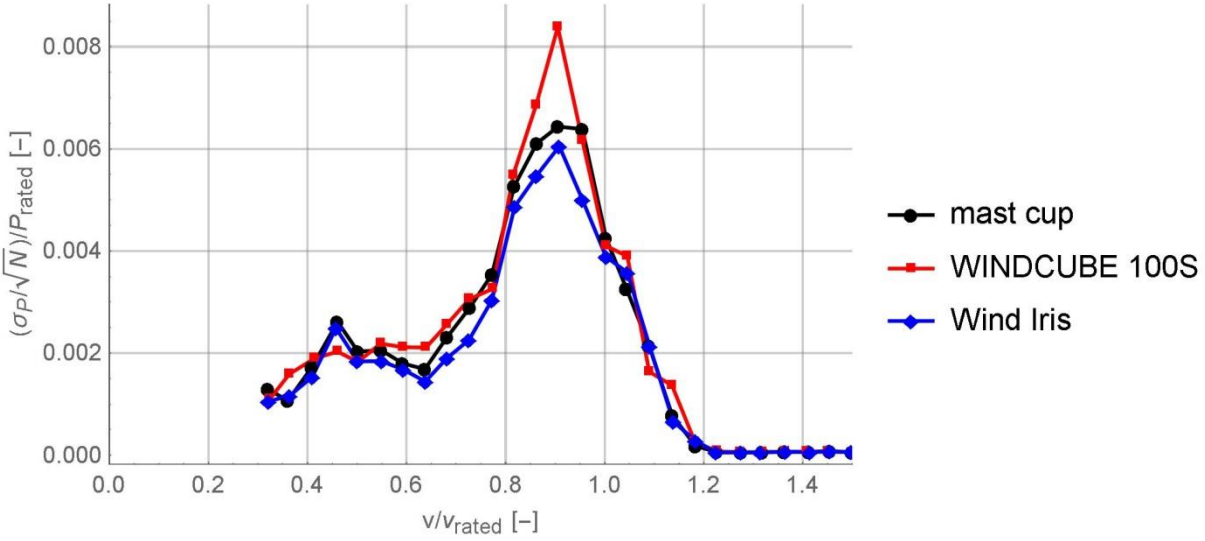

Figure 58 Category A uncertainty in power for the power curve derived from the mast top mounted cup anemometer measurement and the power curve derived from the WINDCUBE 100S horizontal wind speed measurement.

10.2 Category B uncertainty in wind speed

The category B uncertainty in wind speed for the cup anemometer is the combination in quadrature (uncertainty sources considered as independent) of:

- The cup calibration uncertainty – given by the cup anemometer calibration certificate (see certified power curve report [16]), combined with an extra uncertainty term of 0.01/√3*vi to account that Measnet accredited wind tunnels, are within ±1% of each other;
- The cup anemometer class – WindSensor cup anemometer of class A 1.3;
- The data acquisition system uncertainty;
- The uncertainty due to the flow inhomogeneity between the mast position and the turbine position. It was taken as 2% according to the requirements of the IEC 61400-12-1 when the measurements take place in flat terrain within 2 to 3 rotor diameters from the turbine [3].

The category B uncertainty in wind speed for the WINDCUBE 100S is the combination in quadrature (uncertainty sources considered as independent) of:

- The lidar calibration uncertainty – derived from the lidar calibration at Høvsøre (see WINDCUBE 100S calibration report [6]);

- The uncertainty in sensing height error (due to the tilting of the platform)

This uncertainty was quantified as the deviation in wind speed due to the difference between the actual measurement height and hub height, assuming a power law profile with a shear exponent of 0.5. This approach assumes that no information is available about the shear during the measurement campaign and therefore the uncertainty is derived using a rectangular distribution and an extreme value for the shear exponent:

$$u_{v3,i} = \frac{v_{i,m} - v_{i,hub}}{\sqrt{3}}$$

where $V_{i;m}$ is the averaged measured wind speed in bin i and $V_{i;hub}$ the wind speed extrapolated to hub height:

$$v_{i,hub} = v_{i,m}\left(\frac{z_{hub}}{z_{i,m}}\right)^{0.5}$$

with $z_{i;m}$ the averaged measurement height in bin i and z_{hub} the hub height.

- The uncertainty in measurement height due to uncertainty of the inclinometers and scanning head elevation angle estimated at 0.24% of the wind speed;

This uncertainty was estimated assuming it follows a normal distribution. It was converted in wind speed uncertainty assuming the wind profile was following a power law with a shear exponent of 0.2 on average:

$$\frac{u_\varphi}{v} = \left(\frac{H + dH}{H}\right)^{0.2} - 1$$

Where u_φ is the uncertainty in wind speed due to the uncertainty in inclinometers and scanning head elevation angle, v is the wind speed, H is hub height (79.5m) and

$$dH = R.\sin(d\theta_1 + d\theta_2)$$

Where R is the measurement range (272m), $d\theta_1$ is the uncertainty of the inclinometer (estimated at 0.1°) and $d\theta_2$ is the uncertainty of the scanning head elevation angle (estimated at 0.1°) (see calibration report [6]).

- The uncertainty in the measurement height due to the uncertainty in the measurement range, estimated at 0.12% of wind speed;

This uncertainty was assuming the uncertainty in measurement range follows a normal distribution. It was converted in wind speed uncertainty assuming the wind profile was following a power law with a shear exponent of 0.2 on average:

$$\frac{u_R}{v} = \left(\frac{H + dH}{H}\right)^{0.2} - 1$$

Where u_R is the uncertainty in wind speed due to the uncertainty in inclinometers and scanning head elevation angle, v is the wind speed, H is hub height (79.5m) and

$$dH = dR.\sin(\theta_2)$$

Where dR is the measurement range uncertainty, estimated at 2m (see calibration report [6**Error! Reference source not found.**]), θ_1 is the scanning head elevation ngle (14.1°).

- The uncertainty due to the flow inhomogeneity between the mast position and the turbine position (taken as 2% since it is offshore and the lidar measurement volume is at 2.5D from the turbine, by analogy to the requirements of the IEC 61400-12-1 standard for mast measurements [3]).

The category B uncertainty in wind speed for the Wind Iris is the combination in quadrature (uncertainty sources considered as independent) of:

- The lidar calibration uncertainty – derived from the lidar calibration at Høvsøre (see Wind Iris calibration report [5]);

- The uncertainty in sensing height error (due to the tilting of the turbine nacelle) - This uncertainty was quantified in the same way as for the WINDCUBE 100S.

- The uncertainty in measurement height due to the uncertainty of the inclinometers estimated at 0.12% of the wind speed;

This uncertainty was estimated by assuming the inclinometer uncertainty follows a normal distribution. It was converted in wind speed uncertainty assuming the wind profile was following a power law with a shear exponent of 0.2 on average:

$$\frac{u_\varphi}{v} = \left(\frac{H + dH}{H}\right)^{0.2} - 1$$

Where u_φ is the uncertainty in wind speed due to the uncertainty in inclinometers, v is the wind speed, H is hub height (79.5m) and

$$dH = R.\sin(d\theta_1)$$

Where R is the measurement range (265m), $d\theta_1$ is the uncertainty of the inclinometer (estimated at 0.1°) (see calibration report [5]).

- The uncertainty due to the flow inhomogeneity between the mast position and the turbine position (taken as 2% since it is offshore and the lidar measurement volume is at 2.5D from the turbine, by analogy to the requirements of the IEC 61400-12-1 standard for mast measurements [3]).

Figure 59 shows that category B uncertainty in wind speed obtained with the two lidars is higher than that resulting from the standard set up with the top mounted cup anemometer.

It should be noted that contrary to the requirement of the draft revision of the IEC 61400-12-1, no lidar classification uncertainty has been accounted for. This classification scheme is under the process of being finalized by the maintenance team MT12-1 and there is to our knowledge no class number available for sector scanning lidars such as the WINDCUBE 100S in the configuration used in this measurement campaign, nor for nacelle lidars. Nevertheless, it is fair to note that the uncertainty of the lidar can be expected to be a little larger than what is indicated here. For indication, the uncertainty class of a ground based WINDCUBE profiler (WINDCUBE WLS7) is expected to be around 2% [15]. Classification of sector scanning lidar is expected to become available within 2 years, coming along with the publication of the new version of the IEC 61400-12-1 (expected in 2016).

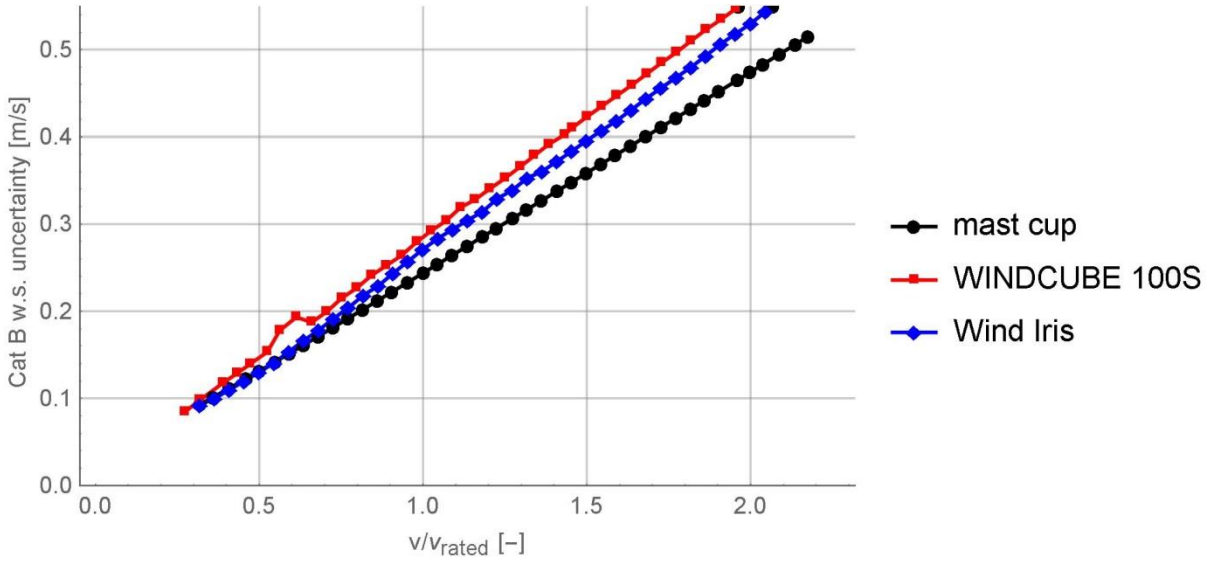

Figure 59 Category B uncertainty in power for the power curve derived from the mast top mounted cup anemometer measurement and the power curve derived from the WINDCUBE 100S horizontal wind speed measurement.

Both for the lidar and the cup anemometer, the category B uncertainty in wind speed is dominated by the 2% uncertainty due to the inhomogeneity between the wind speed measurement location and the turbine location. However, this is identical for both measurement techniques. This uncertainty has therefore been neglected in Figure 60 and Figure 62, in order to ease the comparison to the lidar calibration uncertainty.

Figure 60 shows the remaining uncertainty in wind speed measurement calculated for the Wind Iris. This uncertainty is dominated by the calibration uncertainty and the uncertainty in sensing height. The latter uncertainty is generally derived from a maximum deviation obtained by assuming a shear coefficient of 0.5. The inclinometer uncertainty has a quite marginal contribution.

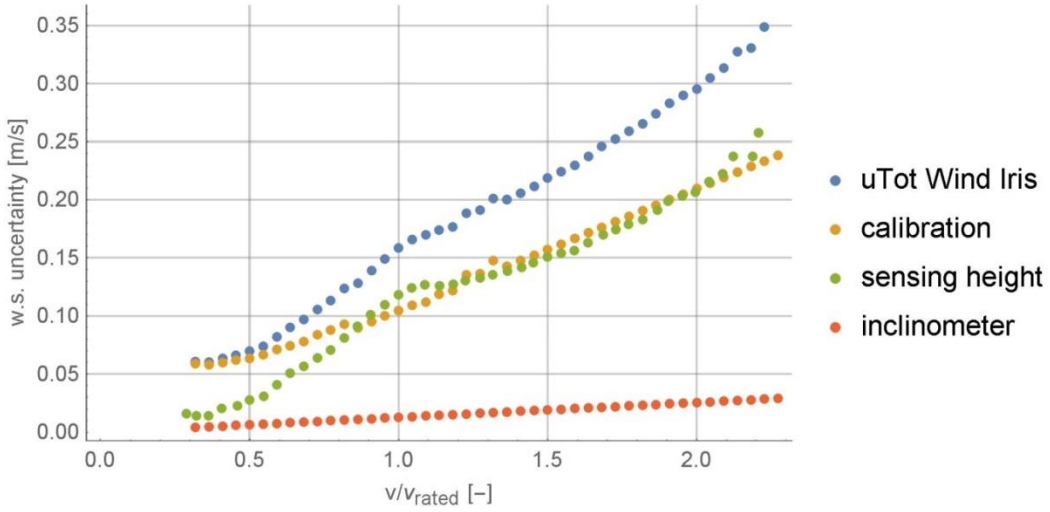

Figure 60 Total wind speed uncertainty of Wind Iris and its various components as a function of wind speed

Similarly, Figure 61 shows the total uncertainty in wind speed measurement calculated for the WINDCUBE 100S. For this lidar, the uncertainty in sensing height is larger than for the Wind Iris since the beam was estimated to measure higher based on the indicated scanner head elevation angle (see

section 7.1). The second dominating term is the calibration uncertainty. The other components have a quite marginal contribution.

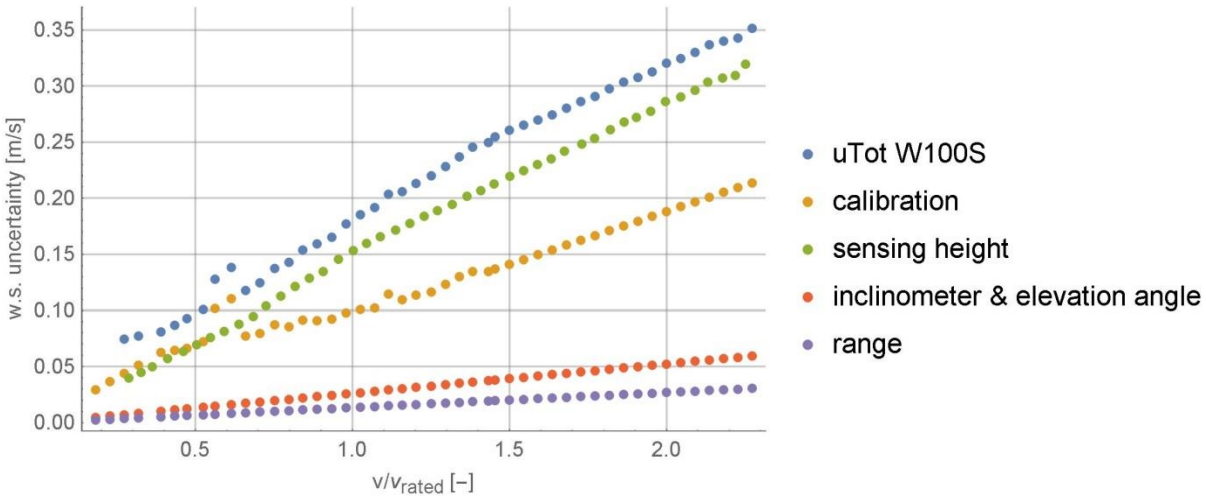

Figure 61 Total wind speed uncertainty of WINDCUBE 100S and its various components as a function of wind speed

Figure 62 and Figure 63 compare, respectively for the WINDCUBE 100S and for the Wind Iris, the uncertainty of the lidar calibration, the total uncertainty of the lidar, the uncertainty of the cup anemometer used for the calibration and uncertainty of the cup used for the power curve measurement. Several observations can be made from these figures:

1) The cup anemometer used for the power curve measurement has a larger uncertainty than the cup anemometer used for the lidar calibration mainly because it has a higher class (class A1.31).
2) As expected, the lidar calibration uncertainty (green) is larger than the reference cup anemometer uncertainty (blue). The reference cup anemometer uncertainty is the combination of the cup anemometer calibration uncertainty, operational uncertainty (Thies First Class anemometers have a class A 0.9 [17]). Nevertheless, the lidar calibration uncertainty is clearly dominated by the reference cup uncertainty (which is itself dominated by the cup anemometer calibration and operational uncertainties). The calibration of the lidar is only provided for the wind speed range 4 to 16m/s; the uncertainty has been assumed to be proportional to the wind speed outside this range. The proportion coefficient between uncertainty and wind speed obtained at 4m/s was applied for wind speed below 4 m/s. The proportion coefficient obtained at 16m/s was applied to wind speeds above 16m/s. This has a relatively small impact on the power curve uncertainty since the rated wind speed is below 16m/s.
3) The calibration uncertainty of the WINDCUBE 100S is slightly larger than the calibration uncertainty of the Wind Iris.
4) However, as mentioned before, the uncertainty in measurement height is larger for the WINDCUBE 100S than for the Wind Iris; which in the end results in larger Category B uncertainty in wind speed.

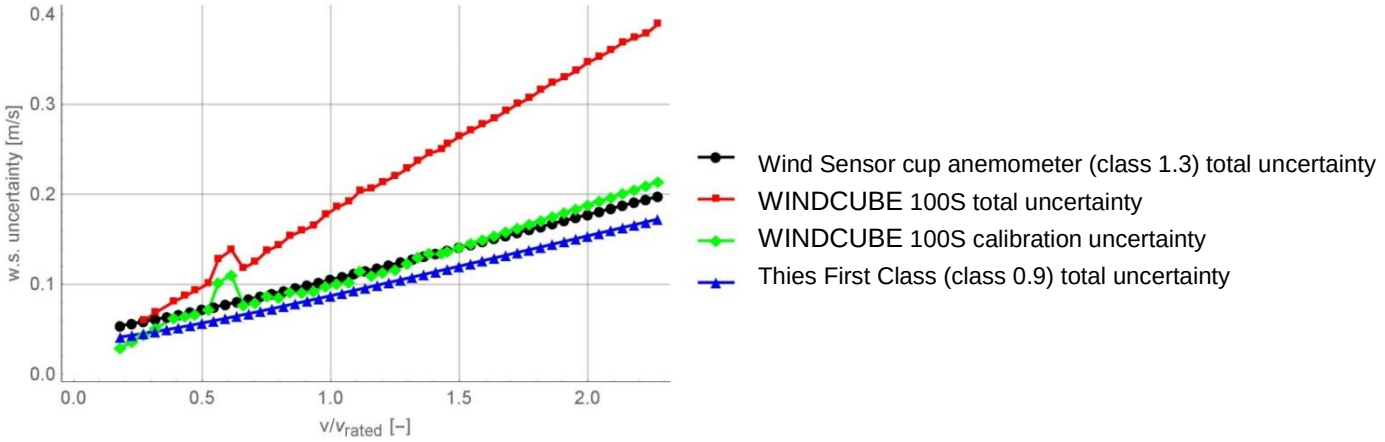

Figure 62 Wind speed measurement uncertainty for the cup anemometer used as reference during the WINDCUBE 100S calibration at Høvsøre (blue) and for the cup anemometer used in the power curve measurement in Greater Gabbard (black), WINDCUBE 100S calibration uncertainty (green); combination of calibration uncertainty, sensing height uncertainty and inclinometer uncertainty for the WINDCUBE 100S (red).

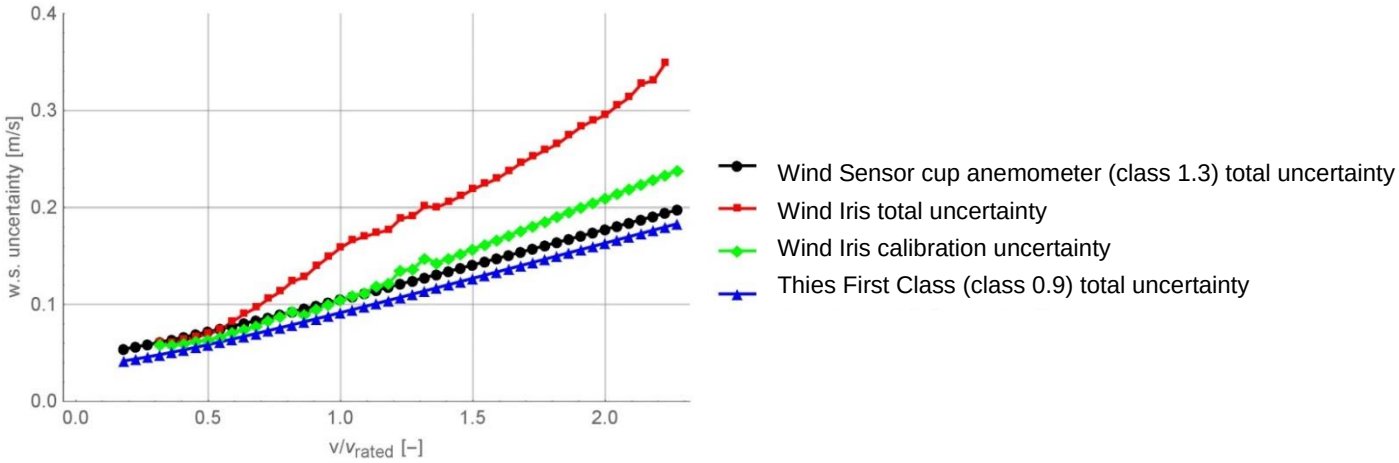

Figure 63 Wind speed measurement uncertainty for the cup anemometer used as reference during the Wind Iris calibration at Høvsøre (blue) and for the cup anemometer used in the power curve measurement in Greater Gabbard (black), Wind Iris calibration uncertainty (green); combination of calibration uncertainty, sensing height uncertainty and inclinometer uncertainty for the Wind Iris (red).

Furthermore, it should be noted that contrary to the requirement of the draft revision of the IEC 61400-12-1, no lidar classification uncertainty has been accounted for. This classification scheme is under the process of being finalized by the maintenance team MT12-1 and there is to our knowledge no class number available for two beam nacelle lidar such as Wind Iris or for sector scanning lidars such as the WINDCUBE 100S in the configuration used in this measurement campaign. Nevertheless, it is fair to note that the uncertainty of the lidar can be expected to be a little larger than what is indicated here.

10.3 Total power curve uncertainty

The total power curve uncertainty is the combination of the category A uncertainty in power and the various category B uncertainties (wind speed, temperature and pressure). The power curve uncertainty is dominated by the category B uncertainty in wind speed and therefore, the difference in category A uncertainty between the lidars and the cup anemometer seen in Figure 58 does not really appear any more in Figure 64. The total power curve uncertainty obtained with the Wind Iris is slightly larger than that obtained with the mast top mounted cup anemometer; and the uncertainty obtained with the WINDCUBE 100S is larger than that obtained with the Wind Iris.

Figure 64 also shows the difference between each lidar power curve and the cup anemometer power curves – difference in power per wind speed bin. The magnitude of this difference is clearly lower than the total power curve uncertainties.

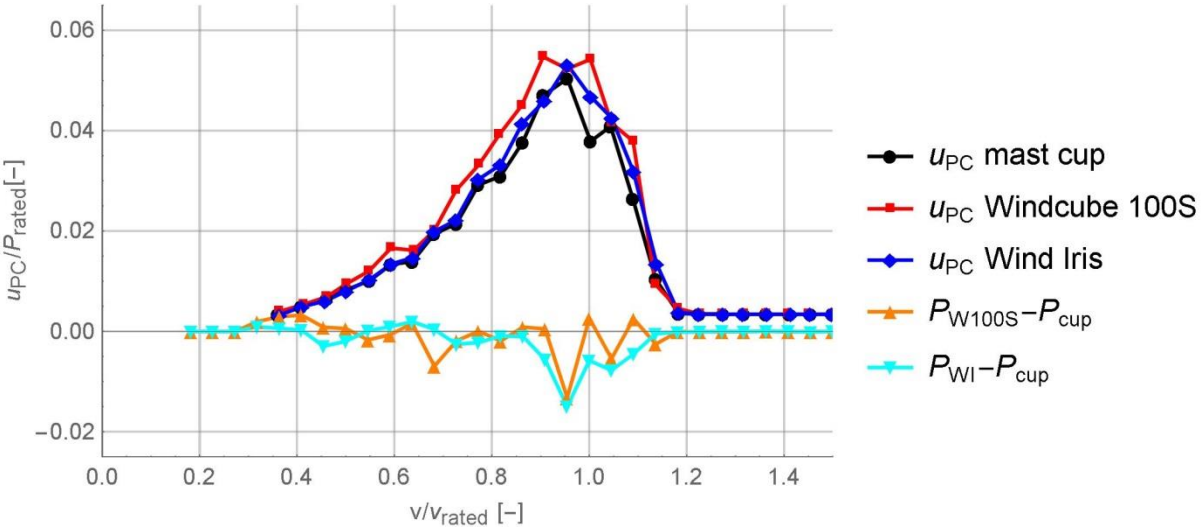

Figure 64 Total power curve uncertainty derived from the mast top mounted cup anemometer measurement and the power curve derived from the WINDCUBE 100S horizontal wind speed measurement and difference between the two power curves.

11. Conclusions

Two lidars, a scanning lidar and a 2 beam nacelle lidar, were deployed simultaneously on an offshore wind turbine in order to assess their performance for power performance verification. The assessment was performed by comparison to measurements taken with the IEC 61400-12-1 standard set up based on a met mast placed at 2.5D from the wind turbine under test. A WINDCUBE 100S, has been deployed on the transition piece platform of the turbine and configured to perform sector scans over a 45° angle right above the met mast. A two beam Wind Iris lidar was installed on the nacelle of the same wind turbine.

One of the main challenges in this measurement campaign has been to set up the measurement height of each lidar. The WINDCUBE 100S was scanning over a fixed arc, defined with a fixed elevation angle and a fixed sector, of 45°. First estimations based on the wind turbine and mast GPS positions and the height of the mast and turbine transition pieces resulted in an elevation angle that was too small to reach the top of the mast. This has been adjusted by performing several sector scans with various elevation angles in order to find the top of the mast. Although it was configured to scan above the top cup anemometer, it remained within 2.6% above hub height for the wind sector used for the power curve measurement. However it should be noted that if the lidar was used without a met mast, the aim would have been to set up the scanning height at the actual turbine hub height, which would only depend on the height difference between the turbine hub and the transition piece platform where the lidar is installed. This height difference is known and the configuration of the lidar would be straight forward.

The optical head of the Wind Iris was inclined in order to account for its height above hub height and the tilting of the turbine nacelle during operation. However this operation has been challenged by the wide motion of the turbine nacelle during deployment. According to the inclinometers readings, the laser beam height has been estimated to be within 1 to 3m higher than hub height at 265m upstream of the rotor.

Nevertheless, since the vertical wind shear was rather low during this measurement campaign, the sensing height error did not significantly affect the lidar 10 minute mean wind speed measurement. However, the related uncertainty, which was derived with a very conservative approach (the same approach was used for both lidars), has increased the final uncertainty significantly for both lidars. A more fair approach would be to estimate this uncertainty using the actual distribution of shear during the campaign. Furthermore, the use of a profiling nacelle lidar (i.e. a lidar that can measure the wind speed at several heights in front of the rotor) could decrease the sensitivity of the results to the inclination of the lidar optical head, since wind speed measurements would anyway be taken below and above the hub height.

The reconstructed horizontal wind speeds from both lidars were in fairly well agreement with the mast top mounted cup anemometer. The wind speed was found to be 0.36% higher than the cup anemometer on average for a wind speed of 10m/s for the Wind Iris, against 0.23% for the WINDCUBE 100S, but the scatter was larger for the scanning lidar. The good comparison of the average wind speed resulted in very similar power curves; the AEP was lower by 0.39% for the WINDCUBE 100S and 0.32% for the Wind iris for an annual average wind speed of 8m/s. The difference between the two power curves was lower than the total power curve uncertainty obtained both for the lidar and cup anemometer. For both lidars the total power curve uncertainty was larger than the cup anemometer power curve uncertainty, larger for the WINDCUBE 100S than for the Wind Iris. This is mainly due to the very large uncertainty in measurement height discussed above. This is believed to be due to challenges in the configuration of the lidars and a very conservative approach. This uncertainty could therefore be reduced by improving the configuration and using a tailored uncertainty that would be fairer to the low shear generally observed offshore. The second dominating uncertainty source is the lidar calibration uncertainty, which is itself dominated by the cup anemometer calibration and operational uncertainties. We therefore believe that lidars can provide an AEP within +/-1% of the AEP obtained with the standard met mast set up and with a total power curve uncertainty within 15% of the cup anemometer power curve uncertainty.

Each of the two lidars used in this measurement campaign present advantages and disadvantages. The Wind Iris has been specifically designed to be mounted on the nacelle of a turbine and to be used for power curve verification. It is relatively easy to deploy, although an installation on the roof of the nacelle remains a very challenging operation. Moreover the nacelle is expected to move significantly, probably even more offshore than onshore. The deployment at Greater Gabbard showed that this motion can make the adjustment of the inclination of the optical head quite difficult. Nevertheless, the Wind Iris measurements compare very well to the cup anemometer and result in a power curve and power curve uncertainty very close to what is obtained with the met mast top mounted cup anemometer.

The WINDCUBE 100S has been designed to be multi-purpose. This can be an asset as the lidar can be used for other purposes than power curve verification. However it also has the disadvantage, for now, not to be provided with an integrated reconstruction algorithm for the horizontal wind speed. The possible deployment on a turbine TP platform on the other hand is easier than on the nacelle. Moreover the TP platform moves significantly less than the nacelle. But, similarly to a met mast, a sector scanning lidar, is always measuring at the same position, contrary to the nacelle mounted lidar that always measure upstream.

12. References

1. Wagner R. et al., Power curve measurement with a nacelle mounted lidar. Wind Energy. 2014, 17(9). 1441–1453. Available: 10.1002/we.1643
2. Wagner and Courtney, Comparison test of WLS200S-22 (Final), DTU Wind Energy LC I-046 (EN)
3. IEC 61400-12-1 Power performance measurements of electricity producing wind turbines, 2005
4. Courtney, Calibrating Nacelle lidars, DTU Wind Energy E-0020
5. Calibration of Avent Wind IRIS lidar SN. E100153, D2.2-part 1, DTU Wind Energy GG I-010 (EN)
6. Calibration of Leosphere W100S, D2.2-part 2, DTU Wind Energy GG I-011 (EN)
7. A4AX-9-K040-00021 5 External Platform Elevation (+)14962 TOS Plan.pdf
8. SSE – IGMMX Instrument Report – 1406-0164 Rev1.2.pdf
9. Vasiljevic N., A time-space synchronization of coherent Doppler scanning lidars for 3D measurements of wind fields, PhD Thesis, 2014, DTU Wind Energy PhD-0027 (EN)
10. Wagner R. et al., *Procedure for wind turbine power performance measurement with a two-beam nacelle lidar*, DTU Wind Energy-E-0019(EN)
11. Wagner R. and S. Davoust, *Nacelle lidar for power curve measurement _ Avedøre campaign*, DTU Wind Energy E-0016(EN)
12. Sathe A, Mann J, Gottschall J, Courtney M. Can Wind Lidars Measure Turbulence? Journal of Atmospheric and Oceanic Technology. 2011;28(7):853-868. Available from: 10.1175/JTECH-D-10-05004.1
13. Wagner R, Sathe A, Mioullet A, Courtney M. Turbulence measurement with a two-beam nacelle lidar. 2013. Poster session presented at European Wind Energy Conference & Exhibition 2013, Vienna, Austria.
14. Mioullet A., Turbulence measurement with two beam nacelle lidar, DTU Wind Energy Master Thesis M-0016.
15. Albers A. et al., Ground-based remote sensor uncertainty – a case study for a wind lidar, EWEA 2013
16. Siemens SWT-3.6MW-107 Power Curve Measurements, D4.1, DTU Wind Energy GG I-013 (EN)
17. Summary of Cup Aneometer Classification, Thies First Class Advanced, Deutsche WindGuard Wind Tunnel Services GmbH, 2008